Abstract

The purpose of this dissertation is to formulate and solve a few problems arising from the impact of a solid body with a fluid. We begin with a simple introductory chapter that establishes an impulsive force from the fluid when impacted from above, and the emergence of a jet up the side of the impacting body. This splash jet is then examined in more detail as we attempt to capture its shape. The dissertation has a central chapter looking a popular application of these problems in the context of stone skipping. After we have considered the jet formation from a horizontal impact we then look at the jet created from a horizontally accelerating vertical plate.

Contents

"Solid Bodies Impacting on Fluids"
Danny Hoskin

1. Introduction

Water entry and impact problems have been of interest throughout history and very relevant in today's modern world. Two key reasons behind the importance of mathematical modelling are shipping and marine structures. Shipping is a theme I will refer to throughout this dissertation.

When reading about water entry and water impact problems I have discovered that this is a vast area of applied mathematics. Therefore I have chosen to look particularly at only a few examples in detail. Firstly I wanted to derive equations for the motion of fluids after an impact from a solid body. For this we look at some examples from [2], solving equations of motion for inviscid fluids. We then use a transformation to solve the problem of an ellipsoid travelling through a fluid and use this result to describe the fluid action at the moment of and impacting body from above. This is of key relevance for many reasons, one could be bow movement on ships, or lowering loads in a water surface.

When beginning this area of research I found two issues that caught my attention. Firstly, the appearance of 'jets' forming at the edges of solid objects upon water entry. We examine this jet looking at the work of Korobkin [14] and find a leading order solution for the profile of the jet. Secondly, I became interested in the idea that when a solid body impacts on the water surface there is an impulsive reaction from the water to the body. This is integral in playing *skipping stones* at the beach (or *Ducks and Drakes* as it is also known). After all, what does make the stone rebound off the water surface? We take a look at skipping stones, numerically solving the equations of motion in order to find domains for skipping involving certain parameters of the problem. We then pose the question of the maximum number of skips.

The idea of objects rebounding off surfaces has had many uses through military history. For example, during cannon warfare at sea the gunners knew that if they hit the water with the correct speed and trajectory then the canon ball would rebound, increase range and hit the underside of opposing ships. This idea was extensively used in the Battle of Trafalgar, see Miloh and Shukron [17] for this and more references. More recently, there was an article in *New Scientist* by Dr. Ian Hutchings [9] about British and German forces using 'bouncing bombs' in the Second World War.

When looking at the ideas of a body entering water from above, it becomes apparent that the instantaneous field of pressure is a key factor in the fluid motion. This then leads me onto another issue, the idea of a vertical wall/plate travelling through a fluid. How is the pressure distributed in this problem? This again is of high significance for shipping. If we imagine a ship travelling through the ocean or being struck by an impacting wave, we need to be sure that the pressure the fluid exerts on the ship can be withstood. For this section of the dissertation we look at the work of King and Needham [11], summarising and extending their work to show the pressure distribution for a vertical plate accelerating horizontally into a fluid.

2. A Rigid Body Impacting on a Fluid Surface

2.1. Introduction to pressure impulse theory

Consider a solid body entering water, for example as we mentioned in the introduction this could be the bow movement of a ship. The question we shall attempt to answer here is 'what happens at the time of impact?'

Firstly we shall make a few assumptions. The fluid is inviscid, the solid object is flat bottomed and parallel to the fluid surface, and the fluid is at rest before the impact. These assumptions lead us to Euler equation,

$$\frac{D\mathbf{u}}{Dt} = -\frac{1}{\rho}\nabla p\,, \tag{2.1}$$

where $\mathbf{u}$ denotes the fluid velocity, t is time, ρ fluid density and p is the fluid pressure, and $\frac{D\mathbf{u}}{Dt} = \frac{\partial \mathbf{u}}{\partial t} + (\mathbf{u}\cdot\nabla)\mathbf{u}$.

During the impact we expect the spatial gradients of velocity to be negligible compared to the $\frac{\partial \mathbf{u}}{\partial t}$ term and so we can approximate (2.1) by,

$$\frac{\partial \mathbf{u}}{\partial t} = -\frac{1}{\rho}\nabla p\,,$$

see [5].

If we integrate the equation above between the time before impact, t_{before}, and the time after impact, t_{after}, we obtain,

$$\mathbf{u}_{after} - \mathbf{u}_{before} = -\frac{1}{\rho}\nabla \int_{t_{before}}^{t_{after}} p\, dt\,,$$

$$\Rightarrow \mathbf{u}_{after} - \mathbf{u}_{before} = -\frac{1}{\rho}\nabla \Pi\,, \tag{2.2}$$

where,

$$\Pi = \int p\, dt\,,$$

is the *pressure impulse*.

If the flow is irrotational we can introduce a velocity potential function in the form, $\mathbf{u} = \nabla\phi$ then from (2.2) we have,

$$\phi_{after} = \phi_{before} - \frac{1}{\rho}\Pi .$$

If the fluid is initially at rest then $\phi_{before} = 0$ and the last equation tells us that the potential, ϕ, is $\left(-\frac{1}{\rho}\right)$ times the pressure impulse needed to generate motion. This is a key point we shall use in Section 2.3.

Also, the i^{th} component of force impulse on a body due to the fluid is given by,

$$-\int_A \Pi n_i \, dA ,$$

where $\mathbf{n}$ is the normal to the body pointing into the fluid, and we integrate over the boundary, A, of the body that is in contact with the fluid.

Now we have a few basic ideas from pressure impulse theory we take a brief digression, looking at the motion of a fluid when an ellipsoid is moving through it.

2.2. An ellipsoid travelling through a still, irrotational and incompressible fluid

We shall now take a brief digression to solve the problem of fluid displacement when there is a solid object moving though it. The solid body we shall look at will be completely submerged in fluid, with the fluid at rest at large distances from the solid body in all directions. Firstly we shall introduce cylindrical coordinates (x, y, φ), taken from [2], where φ is the azimuthal angle about the axis $y = 0$. The set-up of these coordinates is shown below in Figure 2.1.

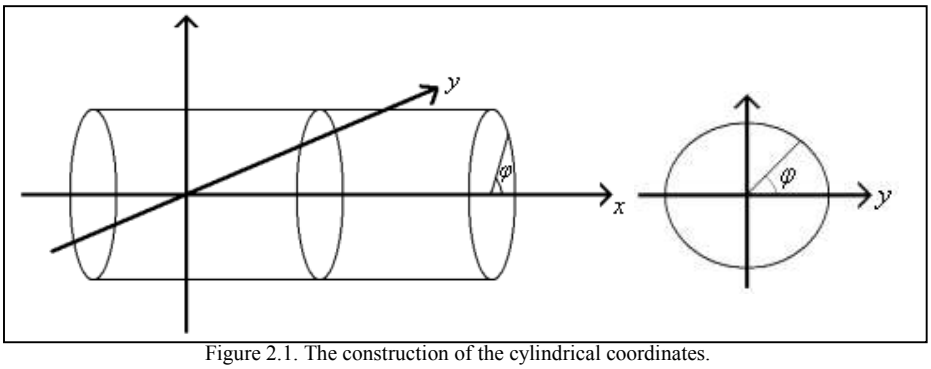

Figure 2.1. The construction of the cylindrical coordinates.

We introduce these coordinates because if the have a shape such as a rectangle defined in the (x, y)-plane rotated fully about the x-axis (to create a cylinder) then we can seek an axisymmetric solution of this object travelling through fluid if it travels purely along the x-axis.

In these coordinates (see Batchelor [2], page 602), for a two-dimensional flow in the (x, y)-plane we have the definitions,

$$\nabla F = \left(\frac{\partial F}{\partial x}, \frac{\partial F}{\partial y} \right), \tag{2.3a}$$

$$\nabla \cdot \mathbf{F} = \frac{\partial F_x}{\partial x} + \frac{1}{y}\frac{\partial}{\partial y}\left(y\, F_y \right), \tag{2.3b}$$

$$\nabla \times \mathbf{F} = \left(0, 0, \frac{\partial F_y}{\partial x} - \frac{\partial F_x}{\partial y} \right). \tag{2.3c}$$

where, $\mathbf{F} = \left(F_x, F_y \right)$.

If we make the assumption that the fluid is irrotational then we can introduce a potential function, ϕ, such that $\nabla \phi = \mathbf{u} = \left(u_x, u_y \right)$. From (2.3a) we can see this will be of the form,

$$u_x = \frac{\partial \phi}{\partial x}, \qquad \text{and,} \qquad u_y = \frac{\partial \phi}{\partial y}. \tag{2.4}$$

Substituting (2.4) into the incompressibility condition,

$$\nabla \cdot \mathbf{u} = 0,$$

gives,

$$\begin{aligned} &\frac{\partial}{\partial x}\left(\frac{\partial \phi}{\partial x} \right) + \frac{1}{y}\frac{\partial}{\partial y}\left(y \frac{\partial \phi}{\partial y} \right) = 0, \\ \Rightarrow\ &\frac{\partial^2 \phi}{\partial x^2} + \frac{\partial^2 \phi}{\partial y^2} + \frac{1}{y}\frac{\partial \phi}{\partial y} = 0. \end{aligned} \tag{2.5}$$

Equation (2.5) gives us a governing equation for ϕ. For one boundary condition we have that the fluid is at rest at large distances away from the object, i.e. $u_x, u_y \to 0$ as $r \to \infty$, where $r = \left(x^2 + y^2 \right)^{1/2}$. From (2.4) this gives, $\phi \to$ constant as $r \to \infty$. Also, on the surface of the object the fluid's velocity matches that of the object, i.e. $\mathbf{n} \cdot \nabla \phi = \mathbf{n} \cdot \mathbf{U}$, where $\mathbf{n}$ is the normal vector to the body, and $\mathbf{U}$ is the body velocity.

Alternatively, since the fluid is incompressible we could introduce a stream-function, ψ, such that the incompressibility condition is satisfied automatically. From (2.3b) we can see that,

$$u_x = \frac{1}{y}\frac{\partial \psi}{\partial y}, \quad \text{and,} \quad u_y = -\frac{1}{y}\frac{\partial \psi}{\partial x}. \tag{2.6}$$

After substituting (2.6) into the irrotational condition, $\nabla \times \mathbf{u} = 0$, we find,

$$\frac{\partial}{\partial x}\left(-\frac{1}{y}\frac{\partial \psi}{\partial x}\right)-\frac{\partial}{\partial y}\left(\frac{1}{y}\frac{\partial \psi}{\partial y}\right)=0,$$

$$\Rightarrow -\frac{1}{y}\frac{\partial^2 \psi}{\partial x^2}-\frac{1}{y}\frac{\partial^2 \psi}{\partial y^2}+\frac{1}{y^2}\frac{\partial \psi}{\partial y}=0,$$

$$\Rightarrow \frac{\partial^2 \psi}{\partial x^2}+\frac{\partial^2 \psi}{\partial y^2}-\frac{1}{y}\frac{\partial \psi}{\partial y}=0. \qquad (2.7)$$

Equation (2.7) gives the governing equation for ψ. The fluid is at rest at large distances from the solid object, so we require $|\mathbf{u}|=\frac{1}{r}|\nabla\psi|\to 0$ as $r\to\infty$. If the object travels in the direction $\mathbf{U}=(U,0)$ then from (2.6), on the surface of the body we require,

$$\frac{1}{y}\frac{\partial \psi}{\partial y}=U, \quad \text{and,} \quad \frac{1}{y}\frac{\partial \psi}{\partial x}=0,$$

and so $\psi=\frac{1}{2}Uy^2$ on the surface of the rigid body.

Instead of a cylinder travelling through fluid we shall now take the case of an oblate ellipsoid that is moving parallel to its axis of revolution using the transformation,

$$x+iy=\left(a^2-b^2\right)^{1/2}\sinh(\xi+i\eta). \qquad (2.8)$$

This transformation creates an ellipse in the (x, y)-plane that we rotate fully about the x-axis to make the ellipsoid, instead of the idea of a rectangle (rotated fully about the x-axis to create a cylinder) that led us to seek the axisymmetric solution (i.e. no φ dependence) governed by the equations (2.5) and (2.7). Figure 2.2 shows the ellipsoid we obtain from the transformation. The ellipsoid moves from left to right in the diagram at constant speed U. As an analogy the reader may like to consider a car tyre moving along an axle. This is a special type of ellipsoid since looking along the x-axis the ellipsoid would appear circular.

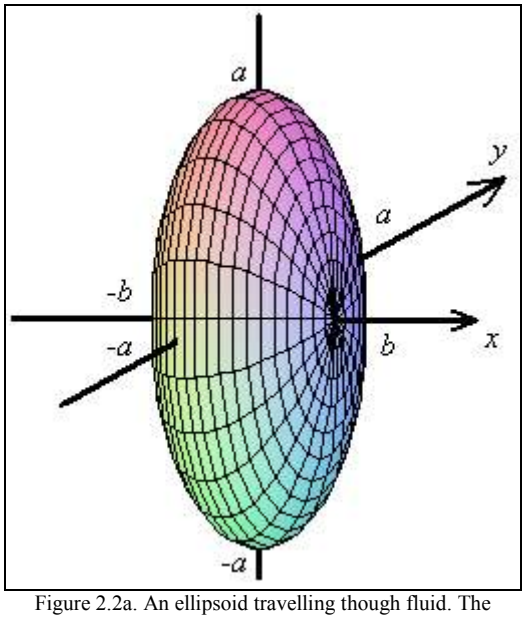

Figure 2.2a. An ellipsoid travelling though fluid. The ellipsoid travels from right to left at a constant speed.

More explicitly (2.8) gives,

$$x = \left(a^2 - b^2\right)^{1/2} \sinh(\xi)\cos(\eta), \tag{2.9a}$$

$$y = \left(a^2 - b^2\right)^{1/2} \cosh(\xi)\sin(\eta). \tag{2.9b}$$

The ellipse drawn out by this transformation is shown below in Figure 2.3. ξ is constant on ellipses drawn centred about the origin.

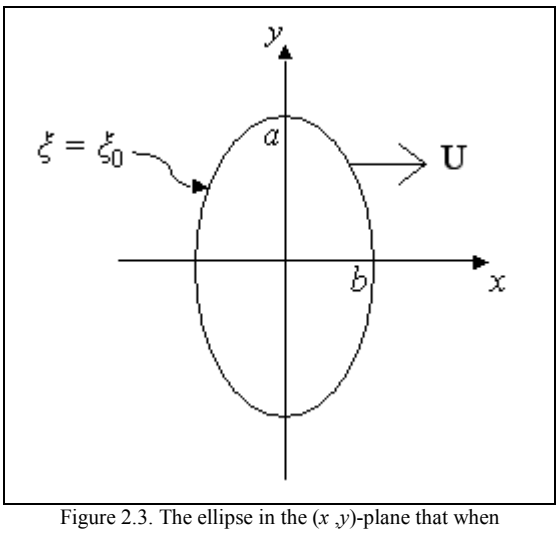

Figure 2.3. The ellipse in the (x ,y)-plane that when rotated about the x-axis creates the ellipsoid in Figure 2.2.

From the transformation the constant value of ξ on the surface of the ellipsoid (ξ_0) is given by,

$$e^{\xi_0} = \left(\frac{a+b}{a-b}\right)^{1/2}, \tag{2.10}$$

since,

$$\left(\frac{x}{\left(a^2-b^2\right)^{1/2}\sinh\left(\xi_0\right)}\right)^2+\left(\frac{y}{\left(a^2-b^2\right)^{1/2}\cosh\left(\xi_0\right)}\right)^2=1,$$

gives,

$$\frac{x^2}{b^2}+\frac{y^2}{a^2}=1.$$

The boundary condition on the surface of the ellipsoid then becomes,

$$\psi=\tfrac{1}{2}U\left(a^2-b^2\right)^{1/2}\cosh^2\left(\xi_0\right)\sin^2\left(\eta\right),$$

since $\psi=\frac{1}{2}Uy^2$ on the free surface - the boundary condition for (2.7).

Using the chain rule and Equations (2.9) we have,

$$\frac{\partial}{\partial x}\equiv\frac{\cosh(\xi)\cos(\eta)}{\left(a^2-b^2\right)^{1/2}\left\{\sinh^2(\xi)+\cos^2(\eta)\right\}}\frac{\partial}{\partial\xi}-\frac{\sinh(\xi)\sin(\eta)}{\left(a^2-b^2\right)^{1/2}\left\{\sinh^2(\xi)+\cos^2(\eta)\right\}}\frac{\partial}{\partial\eta},\quad(2.11a)$$

$$\frac{\partial}{\partial y}\equiv\frac{\sinh(\xi)\sin(\eta)}{\left(a^2-b^2\right)^{1/2}\left\{\sinh^2(\xi)+\cos^2(\eta)\right\}}\frac{\partial}{\partial\xi}+\frac{\cosh(\xi)\cos(\eta)}{\left(a^2-b^2\right)^{1/2}\left\{\sinh^2(\xi)+\cos^2(\eta)\right\}}\frac{\partial}{\partial\eta}.\quad(2.11b)$$

Also, from (2.4) and (2.6) we have,

$$\frac{\partial\phi}{\partial x}=\frac{1}{y}\frac{\partial\psi}{\partial y},\qquad\text{and,}\qquad(2.12a)$$

$$\frac{\partial\phi}{\partial y}=-\frac{1}{y}\frac{\partial\psi}{\partial x}.\qquad(2.12b)$$

Using (2.11), Equation (2.12a) becomes,

$$\cosh(\xi)\cos(\eta)\frac{\partial\phi}{\partial\xi}-\sinh(\xi)\sin(\eta)\frac{\partial\phi}{\partial\eta}=\frac{1}{y}\left[\sinh(\xi)\sin(\eta)\frac{\partial\psi}{\partial\xi}+\cosh(\xi)\cos(\eta)\frac{\partial\psi}{\partial\eta}\right],\qquad(2.13)$$

and Equation (2.12b) becomes,

$$\sinh(\xi)\sin(\eta)\frac{\partial\phi}{\partial\xi}+\cosh(\xi)\cos(\eta)\frac{\partial\phi}{\partial\eta}$$
$$=-\frac{1}{y}\left[\cosh(\xi)\cos(\eta)\frac{\partial\psi}{\partial\xi}+-\sinh(\xi)\sin(\eta)\frac{\partial\psi}{\partial\eta}\right]. \quad (2.14)$$

If we divide (2.13) by $\sinh(\xi)\sin(\eta)$, and (2.14) by $\cosh(\xi)\cos(\eta)$, and then add the two results together we obtain,

$$\frac{\partial\phi}{\partial\xi}=\frac{1}{\sigma}\frac{\partial\psi}{\partial\eta}. \quad (2.15)$$

If we divide (2.13) by $\cosh(\xi)\cos(\eta)$, and (2.14) by $\sinh(\xi)\sin(\eta)$, and then subtract the two results we obtain,

$$\frac{\partial\phi}{\partial\eta}=-\frac{1}{y}\frac{\partial\psi}{\partial\xi}. \quad (2.16)$$

Recall that y was given by Equation (2.9b). Equations (2.15) and (2.16) give us a relationship between the potential function and the stream function in our elliptic coordinate system. We do not need to transform both governing equations, (2.5) and (2.7), for ϕ and ψ. We can solve either of these, with their associated boundary conditions, and use the relations we have just found to find the other. We shall choose to solve for the stream function, governing equation (2.7), since we have a simpler inner boundary condition.

Recall that the boundary condition on the free surface for (2.7) was given by $\psi=\frac{1}{2}Uy^2$. Using (2.9b) and (2.10) we have the surface condition,

$$\psi=\tfrac{1}{2}U\left(a^2-b^2\right)\cosh^2(\xi)\sin^2(\eta), \quad \text{when} \quad \xi=\xi_0.$$

This leads us to seek a solution of the form $\psi=F(\xi)\sin^2(\eta)$. Using this form of ψ with (2.11) and (2.7) we obtain,

$$F''(\xi)\cosh(\xi)-F'(\xi)\sinh(\xi)-2F(\xi)\cosh(\xi)=0.$$

(The details of this stage are moved to A1 of the Appendix). We have arrived at an ordinary differential equation with the general solution,

$$F(\xi)=A\cosh^2(\xi)+B\left(\tan^{-1}\left(\frac{1}{\sinh(\xi)}\right)\cosh^2(\xi)-\sinh(\xi)\right). \quad (2.17)$$

where A and B are arbitrary constants.

One of the boundary conditions for the flow was that, as we move away from the ellipsoid, the fluid is at rest. From (2.6) this translates as $\psi\to$ constant as $\xi\to\infty$. In

this limit the second term of (2.17) tends to zero, and the first term tends to infinity. Hence we must have $A = 0$ in order to satisfy this condition. The surface condition $\psi = \frac{1}{2}U\left(a^2 - b^2\right)\cosh^2(\xi)\sin^2(\eta)$ when $\xi = \xi_0$ gives $F(\xi_0) = \frac{1}{2}U\left(a^2 - b^2\right)\cosh^2(\xi_0)$ as the other boundary condition for (2.17). Since we have established that $A = 0$, the condition gives,

$$B\tan^{-1}\left(\frac{1}{\sinh(\xi_0)}\right)\cosh^2(\xi_0) - \sinh(\xi_0) = \frac{1}{2}U\left(a^2 - b^2\right)\cosh^2(\xi_0),$$

$$\Rightarrow B = \frac{\frac{1}{2}U\left(a^2 - b^2\right)\cosh^2(\xi_0)}{\tan^{-1}\left(\frac{1}{\sinh(\xi_0)}\right)\cosh^2(\xi_0) - \sinh(\xi_0)}.$$

Now, from (2.10) we have,

$$\sinh(\xi_0) = \frac{b}{\left(a^2 - b^2\right)^{1/2}}, \qquad \text{and,} \qquad \cosh(\xi_0) = \frac{a}{\left(a^2 - b^2\right)^{1/2}},$$

and so,

$$B = \frac{\frac{1}{2}Ua^2\left(a^2 - b^2\right)}{a^2\tan^{-1}\left(\frac{\left(a^2 - b^2\right)^{1/2}}{b}\right) - b\left(a^2 - b^2\right)^{1/2}}.$$

From simple trigonometry on a right-angled triangle, $\tan^{-1}\left(\frac{\left(a^2 - b^2\right)^{1/2}}{b}\right) = \cos^{-1}(b/a)$

and so we have the solution,

$$\psi = \frac{\frac{1}{2}Ua^2\left(a^2 - b^2\right)\sin^2(\eta)}{b\left(a^2 - b^2\right)^{1/2} - a^2\cos^{-1}(b/a)}\left\{\sinh(\xi) - \cosh^2(\xi)\tan^{-1}\left(\frac{1}{\sinh(\xi)}\right)\right\}. \quad (2.18)$$

2.3. A solid object contacting a fluid surface

In the last section we found the solution of an ellipsoid moving steadily through a fluid. If we take the limiting case of this example when $b = 0$, we obtain the motion from a round plate travelling through the fluid, with a radius of *a*, moving along the *x*-axis in Figure 2.2. At the moment of a solid impacting on the fluid from above at speed *U* we have the same type of motion we have if the *x*-axis points vertically down wards, this is shown in Figure 2.4 below.

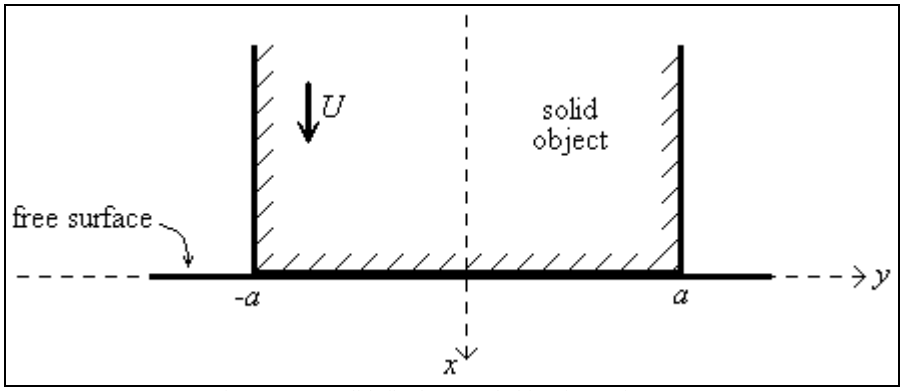

Figure 2.4. A solid, flat-bottomed object impacting on a fluid surface. The underside of the body is circular.

In this limit the stream function, Equation (2.18), reduces to,

$$\psi = -\frac{a^2 U}{\pi}\left\{\sinh(\xi) - \cosh^2(\xi)\tan^{-1}\left(\frac{1}{\sinh(\xi)}\right)\right\}\sin^2(\eta). \tag{2.19}$$

Using the stream function we can obtain the shape of the fluid surface at the moment of contact. On the free surface we have $x = 0$. From (2.9a) this is equivalent to $\eta = \frac{1}{2}\pi$. Recall that from (2.6) we have,

$$u_x = \frac{1}{y}\frac{\partial \psi}{\partial y}, \quad \text{and,} \quad u_y = -\frac{1}{y}\frac{\partial \psi}{\partial x}. \tag{2.20}$$

Hence,

$$u_y = \left(-\frac{1}{y}\frac{\partial \psi}{\partial x}\right)_{x=0} = -\frac{1}{y}\left(\frac{\partial \psi}{\partial \xi}\frac{\partial \xi}{\partial x} + \frac{\partial \psi}{\partial \eta}\frac{\partial \eta}{\partial x}\right)_{\eta=\frac{1}{2}\pi}$$

which is equal to zero from (2.11) and (2.19). Therefore we have a free surface fluid velocity purely in the vertical direction in Figure 2.4. For the other component of velocity from (2.20) along with (2.9), (2.11) and (2.19) we obtain,

$$\begin{aligned} u_x &= \left(\frac{1}{y}\frac{\partial \psi}{\partial y}\right)_{x=0} = \frac{1}{y}\left(\frac{\partial \psi}{\partial \xi}\frac{\partial \xi}{\partial y} + \frac{\partial \psi}{\partial \eta}\frac{\partial \eta}{\partial y}\right)_{\eta=\frac{1}{2}\pi} \\ &= \frac{1}{y}\left(\frac{\partial \psi}{\partial \xi}\frac{\sinh(\xi)\sin(\eta)}{a\{\sinh^2(\xi)+\cos^2(\eta)\}} + \frac{\partial \psi}{\partial \eta}\frac{\cosh(\xi)\cos(\eta)}{a\{\sinh^2(\xi)+\cos^2(\eta)\}}\right)_{\eta=\frac{1}{2}\pi} \\ &= -\frac{2aU}{\pi y}\left(\coth(\xi) - \cosh(\xi)\tan^{-1}\left(\frac{1}{\sinh(\xi)}\right)\right) \\ &= -\frac{2U}{\pi}\left(\frac{1}{\sinh(\xi)} - \tan^{-1}\left(\frac{1}{\sinh(\xi)}\right)\right) \end{aligned}$$

Also, from (2.9) we have,

$$\left(\frac{y^2}{a^2}-1\right)^{-\frac{1}{2}} = \left(\frac{a^2\cosh^2(\xi)\sin^2(\eta)}{a^2}-1\right)^{-\frac{1}{2}} = \left[\sinh^2(\xi)\right]^{-\frac{1}{2}} = \frac{1}{\sinh(\xi)}$$

when $b=0$, and $\eta = \frac{1}{2}\pi$. And so,

$$u_x = -\frac{2U}{\pi}\left(\left(\frac{y^2}{a^2}-1\right)^{-\frac{1}{2}} - \tan^{-1}\left(\left(\frac{y^2}{a^2}-1\right)^{-\frac{1}{2}}\right)\right). \tag{2.21}$$

Figure 2.5 below shows the velocity of the free surface at the moment of impact using (2.21). The diagram shows only the right-hand side of the impact, but there is a line of symmetry along the *x*-axis.

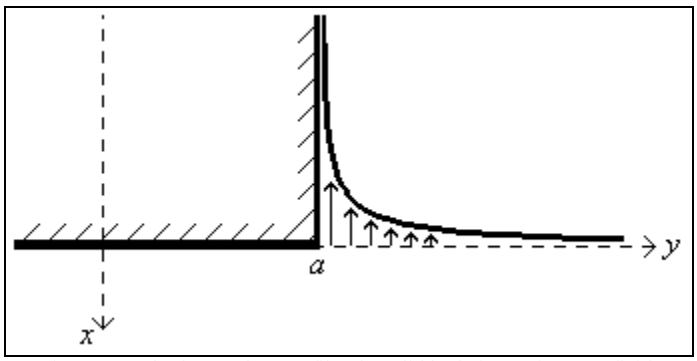

Figure 2.5. The free surface profile of a solid body impacting on a fluid.

Figure 2.5 shows asymptotic behaviour for the free surface profile as it approaches the solid body. Clearly in a physical case we would have a finite amount of fluid and so could not have asymptotic behaviour. We will examine this splash more closely in Section 3 and show the appearance jets forming in this region.

Recall that from section 2.1 we stated that the force impulse was given by,

$$-\int \Pi n_i \, dA \,,$$

where **n** is the normal to the body pointing into the fluid. From Figure 2.4 the normal points directly down the *x*-axis (which increases downward). So the force impulse is directed upward in Figure 2.4, i.e. against the motion of the solid object.

We can therefore work out the force impulse for the object in Figure 2.4. Recall that the under surface of the solid body is a circular disc of radius *a*, and also $\Pi = -\rho\phi$ from Section 2.1, and so the force impulse is given by,

$$2\pi\int_0^a (\Pi)_{x=0}\, r\, dr = -2\pi\rho\int_0^a (\phi)_{x=0}\, r\, dr \,. \tag{2.22}$$

where *r* is the radius of the disc.

From (2.9b) and (2.10) and Figure 2.3, $r = a\sin(\eta)$ for $0 \le \eta \le \pi/2$ on the surface of the solid body. Also from (2.19),

$$\frac{\partial \psi}{\partial \xi} = -\frac{a^2 U}{\pi}\left\{2\cosh(\xi) - 2\sinh(\xi)\cosh(\xi)\tan^{-1}\left(\frac{1}{\sinh(\xi)}\right)\right\}\sin^2(\eta),$$

which becomes,

$$\left(\frac{\partial \psi}{\partial \xi}\right)_{\xi=\xi_0} = -\frac{2a^2 U}{\pi}\sin^2(\eta),$$

on the free surface. Hence from (2.16),

$$\frac{\partial \phi}{\partial \eta} = -\frac{1}{y}\frac{\partial \psi}{\partial \xi} = \frac{2aU}{\pi}\sin(\eta),$$
$$\Rightarrow \phi = -\frac{2aU}{\pi}\cos(\eta).$$

The force impulse on the solid from the fluid is then given by

$$4a^2 U\rho\int_0^a \cos(\eta)\sin(\eta)\,dr = 4a^3 U\rho\int_0^{\pi/2}\cos^2(\eta)\sin(\eta)\,d\eta$$
$$= 4a^3 U\rho\left[\frac{\cos^3(\eta)}{3}\right]_0^{\pi/2} = \frac{4a^3 U\rho}{3}.$$

from (2.22). An interesting question is to ask is, "if this force impulse was high enough, could it make the object rebound off the fluid surface?" In reality this is possible and in section 4 we take a closer look at the game of *Skipping Stones*.

3. Jets

3.1. The impact of a box-like structure on a fluid of small depth

In the last section we found that when a solid body enters fluid there is an associated splash at the edge of that body. The analysis suggested asymptotic behaviour for this splash up the side of the body, which is clearly not realistic. In reality a jet emerges in this part of the fluid, and we pick up the work of Alexander Korobkin [14] to examine this jet.

As in section 2 we shall concern ourselves with the simpler shape of a box-like structure impacting on an incompressible (and inviscid) fluid at rest. However, this time we shall add in a solid surface at the bottom on the fluid, giving the fluid a specified depth. We shall make the assumption that the depth of the fluid is significantly smaller than the length of the bottom of the solid box. In real terms this could be a simple model for a ship in a docking situation. This assumption will give rise to a small parameter $\varepsilon = h/L$, where h is the depth of the fluid and L is half the length of the solid body, which we shall use later in this section. We shall concern ourselves with the moment immediately after impact in which we have a jet emerging. The set-up of the problem is shown below in Figure 3.1.

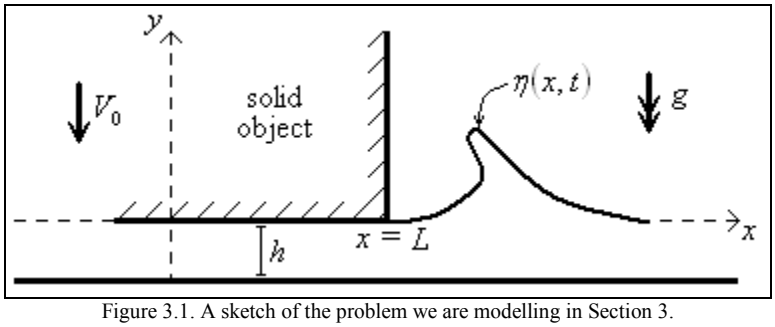

Figure 3.1. A sketch of the problem we are modelling in Section 3.
We have a solid box-like structure entering a fluid that is at rest.

From Figure 3.1 we have the (x, y)-axes positioned such that $x = 0$ straight down the centre of the object where we expect a line of symmetry. $y = 0$ is the free surface position before impact, and the fluid bed is at $y = -h$. We shall let $y = \eta(x,t)$ describe the shape of the free surface, where t is time. The density of the fluid is assumed constant and given by ρ_0. Initially the fluid domain is given by $-\infty < x < \infty$ and $-h < y < 0$. V_0 and g relate to the constant speed of the solid body and the acceleration due to gravity respectively. Both of these constants are assumed to remain constant throughout the process.

The fluid in Figure 3.1 must satisfy the Euler equations given by,

$$\frac{\partial u}{\partial t}+u\frac{\partial u}{\partial x}+v\frac{\partial u}{\partial y}=-\frac{1}{\rho_0}\frac{\partial p}{\partial x}, \qquad \text{and,} \tag{3.1a}$$

$$\frac{\partial v}{\partial t}+u\frac{\partial v}{\partial x}+v\frac{\partial v}{\partial y}=-\frac{1}{\rho_0}\frac{\partial p}{\partial y}-g, \tag{3.1b}$$

along with the compressibility condition,

$$\frac{\partial u}{\partial x}+\frac{\partial v}{\partial y}=0, \tag{3.2}$$

where $\mathbf{u}=(u,v)$ is the usual velocity vector, and p is pressure. Since we have stated we are looking at an irrotational fluid,

$$\frac{\partial u}{\partial y}=\frac{\partial v}{\partial x}, \tag{3.3}$$

must also be satisfied. On the underside of the solid body we must have that the normal velocity component is the same as that of the box and so,

$$v=-V_0, \qquad \text{when,} \quad y=-V_0 t, \quad \text{and,} \quad -L<x<L, \tag{3.4}$$

because the position of the underside of the solid body is $y=-V_0 t$ at a given time, t. On the fluid bed we have that there is no normal flow through the solid wall. Hence,

$$v=0, \qquad \text{where,} \quad y=-h, \quad \text{and,} \quad -\infty<x<\infty. \tag{3.5}$$

If we define $\mu(x,y,t)=y-\eta(x,t)$. Then μ remains zero on the free surface and so,

$$\frac{D\mu}{Dt}=\frac{\partial \mu}{\partial t}+(\mathbf{u}\cdot\nabla)\mu=0, \qquad \text{on,} \qquad y=\eta(x,t).$$

From the definition of μ we have,

$$\frac{\partial \mu}{\partial t}=-\frac{\partial \eta}{\partial t}, \quad \frac{\partial \mu}{\partial x}=-\frac{\partial \eta}{\partial x}, \quad \text{and,} \quad \frac{\partial \mu}{\partial y}=1,$$

and so on the free surface, $y=\eta(x,t)$, we have the kinematic condition,

$$\frac{\partial \eta}{\partial t}+u\frac{\partial \eta}{\partial x}=v. \tag{3.6}$$

Also on the free surface we shall set,

$$p=0. \tag{3.7}$$

In order to solve this problem we shall split the fluid domain into six sections, with the solutions for each sections matching where they are in contact with each other. The sections are shown in Figure 3.2.

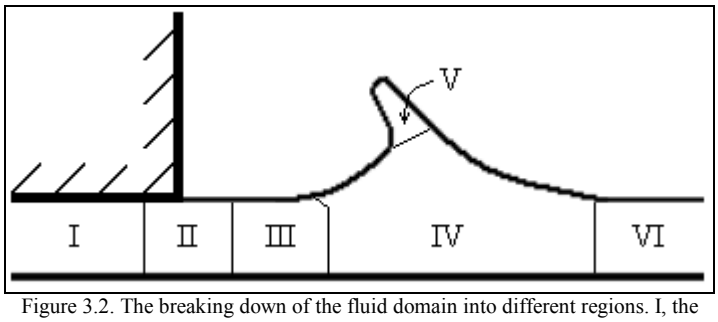

Figure 3.2. The breaking down of the fluid domain into different regions. I, the area beneath the solid body. II, the area close to the bottom edge of the solid body. III, region of inertial flow. IV, the jet root. V, the splash. VI, the outer region.

In reality region II, the area close to the bottom edge of the solid, is very thin in the *x*-direction and *x* is $O(h)$. Korobkin [14] notes that the solution in this region, to first order, is trivial and therefore does not provide any additional matching conditions. We can then match regions I and III together and neglect region II. We need only solve the problem for $x > 0$ since we have already stated that the solution is symmetric about the *y*-axis.

3.2. Region I: Flow between the solid body and the fluid bed

Let us begin by estimating the size of each of the terms in the problem. In region I we expect, *x* is $O(L)$, *y* is $O(h)$, *t* is $O(h/V_0)$, and *v* is $O(V_0)$. From Equation (3.2) we then have $u = O(LV_0/h)$, and from Equation (3.1a) we have $p = O(\rho_0 V_0^2 \varepsilon^{-2})$ to leading order and is a function of *x* and *t*. From Equation (3.3), $\partial u/\partial y = 0$ to leading order, and so *u* is a function of only *x* and *t*.

To leading order the flow is then given by the solution to the equations (from (3.1) and (3.2)),

$$\frac{\partial u}{\partial t} + u\frac{\partial u}{\partial x} = -\frac{1}{\rho_0}\frac{\partial p}{\partial x}, \tag{3.8}$$

$$\frac{\partial u}{\partial x} + \frac{\partial v}{\partial y} = 0, \tag{3.9}$$

where, $u = u(x,t)$, $p = p(x,t)$ and $v = v(x,y,t)$. The boundary conditions (3.4) and (3.5) remain the same. If we match the pressure in region I and region III then from (3.7) we also have,

$$p = 0, \qquad \text{when} \qquad x = L. \tag{3.10}$$

Since the flow is symmetrical in the *y*-axis we must also have,

$$u = 0, \qquad \text{for,} \qquad x = 0, \quad \text{and,} \quad -h < y < -V_0 t. \tag{3.11}$$

If we integrate (3.9) with respect to x and y and apply the conditions, (3.4), (3.5) and (3.11) we obtain,

$$u(x,t) = \frac{V_0 x}{h - V_0 t}. \tag{3.12}$$

If we then substitute (3.12) back into (3.9), we can then integrate with respect to y and apply (3.5) to give,

$$v(x,y,t) = -V_0 \frac{(h+y)}{(h - V_0 t)}. \tag{3.13}$$

From (3.13) we can see that, to leading order, in this region v does not depend on x. This is only for the case we are examining where the solid body has constant velocity through the fluid. A diagram of the fluid velocity field is shown in Figure 3.3 below.

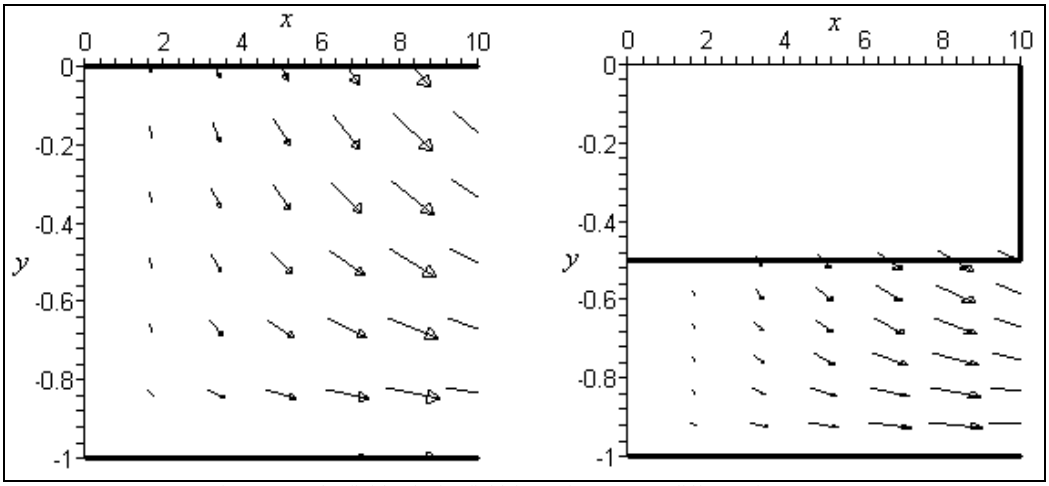

Figure 3.3. The fluid velocity field for region I at two different time steps. The first picture shows the fluid velocity closely after impact, while the second shows the velocity field when the solid body is halfway to the fluid bed and the original free surface.

To create Figure 3.3, the parameters were given the values; $V_0 = 1\text{ms}^{-1}$, $h = 1\text{m}$ and $L = 10\text{m}$, giving the duration from impact until solid body and fluid bed contact as $0 < t < 1$. Figure 3.3 shows how the fluid is pushed out from the side from beneath the solid body.

Substituting (3.12) into (3.8) gives,

$$\frac{\partial p}{\partial x} = -\frac{2\rho_0 V_0^2 x}{(h - V_0 t)^2},$$

which after integrating and application of (3.10) gives,

$$p(x,t)=\frac{\rho_0 V_0^2}{(h-V_0 t)^2}\left(L^2-x^2\right). \tag{3.14a}$$

A diagram of this pressure distribution is shown below in Figure 3.4.

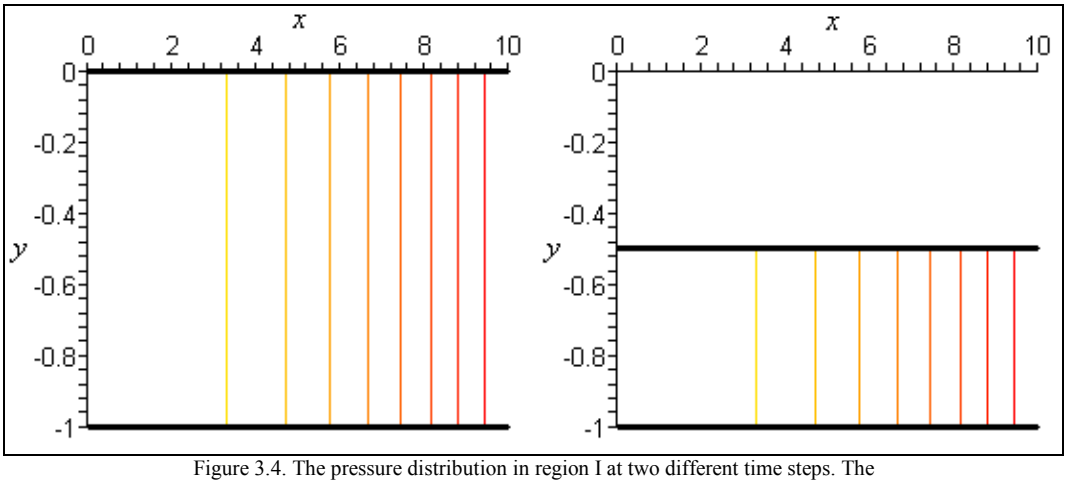

Figure 3.4. The pressure distribution in region I at two different time steps. The first picture is immediately after impact, and second is when the solid body is half way between the original free surface and the fluid bed. The yellow contours show high pressure and the red contours show low pressure.

Figure 3.4 shows the pressure contours for the flow in Figure 3.3. We can see the high pressure below the centre of the solid body. This is to be expected since the fluid is being pushed out through the side.

Recall that we created the small parameter $\varepsilon = h/L$. We can express (3.14a) with this parameter as,

$$p(x,t)=\rho_0 V_0^2 \varepsilon^{-2}(h-V_0 t)^{-2}\left(1-\frac{x^2}{L^2}\right), \tag{3.14b}$$

which is unbounded as $\varepsilon \to 0$, i.e. when the box approaches the fluid bed at $t = h/V_0$.

As an interesting side note can we can work out the hydrodynamic force on the solid body. The force, F is given by integrating (3.14a) over the underside of the box-like shape [7].

$$F(t)=\int_{-L}^{L}\frac{\rho_0 V_0^2}{(h-V_0 t)^2}\left(L^2-x^2\right)dx=\frac{\rho_0 V_0^2}{(h-V_0 t)^2}\left[L^2 x-\frac{x^3}{3}\right]_{-L}^{L},$$
$$\Rightarrow F(t)=\tfrac{4}{3}\rho_0 V_0^2 L^3 (h-V_0 t)^{-2}. \tag{3.15}$$

The solid body approaches the fluid bed as $t \to h/V_0$. In this limit, both (3.14) and (3.15), i.e. the pressure in the fluid and the force in the solid body, tend to infinity and so the solution breaks down in this limit. Also, keeping $V_0 = \text{constant}$ in a practical

experiment requires an unrealistically large force as $t \to h/V_0$. In practice V_0 will decrease with time.

3.3. Region III: Inertial flow

We now move on to region III, matching the flow to that in region I. The flow in this region is termed *inertial* since from the dynamic boundary condition (3.7) the pressure is zero at leading order. The orders of the variables are the same as in region I. We would expect that the flow is approximately one-dimensional and dependent on the flow out of region I. In this region (3.1) and (3.2) become,

$$\frac{\partial u}{\partial t} + u\frac{\partial u}{\partial x} = 0\,, \tag{3.16}$$

$$\frac{\partial u}{\partial x} + \frac{\partial v}{\partial y} = 0\,, \quad \text{where,} \quad L < x < c(t)\,, \quad \text{and,} \quad -h < y < \eta(x,t)\,. \tag{3.17}$$

Here, $c(t)$ gives a measure of the boundary between regions III and IV. We also have the kinematic condition that was given by (3.6), so,

$$\frac{\partial \eta}{\partial t} + u\frac{\partial \eta}{\partial x} = v\,, \qquad \text{when,} \qquad L < x < c(t)\,, \quad \text{and,} \qquad y = \eta(x,t)\,. \tag{3.18}$$

From (3.5) we also have,

$$v = 0\,, \qquad \text{when,} \qquad L < x < c(t)\,, \quad \text{and,} \qquad y = -h\,. \tag{3.19}$$

If we are to match the solution for region III to that of region I then we must have,

$$\eta(x,t) = -V_0 t\,, \qquad \text{when,} \qquad x = L\,, \tag{3.20}$$

and also from (3.12),

$$u(L,t) = \frac{V_0 L}{h - V_0 t}\,. \tag{3.21}$$

The solution of (3.16) which satisfies (3.21) is given by,

$$u(x,t) = \frac{V_0(2L - x)}{h - V_0 t}\,, \qquad \text{for,} \quad L < x < c(t)\,. \tag{3.22}$$

Substituting (3.22) into (3.17) gives,

$$\frac{\partial v}{\partial y} = \frac{V_0}{h - V_0 t} \Rightarrow v = \frac{V_0 y}{h - V_0 t} + f(x,t)\,,$$

where f is an arbitrary function of x and t. Applying (3.19) gives,

$$v = \frac{V_0}{h - V_0 t}(h + y). \tag{3.23}$$

Substituting (3.22) and (3.23) into (3.18) gives,

$$\eta_t + \frac{V_0(2L - x)}{h - V_0 t}\eta_x = \frac{V_0}{h - V_0 t}(h + \eta), \quad \text{and,} \quad L < x < c(t), \tag{3.24}$$

which must be solved with the boundary condition (3.20). The solution of this problem is,

$$\eta(x,t) = L^2 \frac{h - V_0 t}{(2L - x)^2} - h, \quad \text{where,} \quad L < x < c(t). \tag{3.25}$$

Figure 3.5 shows the velocity filed and the free surface profile given by (2.35) for region III.

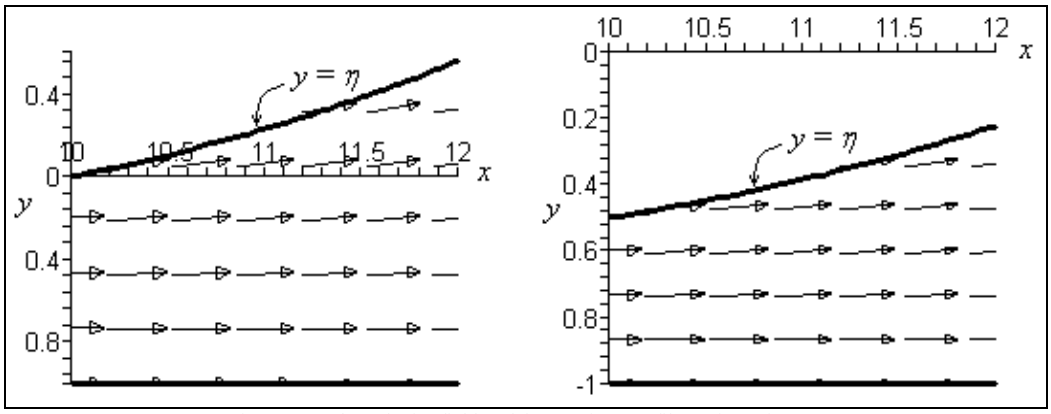

Figure 3.5. The velocity field and free surface profile, η, in region III.
The first picture is immediately after impact and the second is when
the solid body is halfway between the original free surface and the fluid bed.

To create Figure 3.5 we have temporarily fixed $c(t) = 12\text{m}$, we will find the true value of this in section 3.4. Figure 3.5 shows what happened to the fluid after it has been forced out from below the solid object as in Figure 3.3. The free surface appears to be forced upwards from the corner of the solid body.

3.4. Region IV: The base of the jet

The key part of region III is the location of $c(t)$. To examine region IV we shall use a moving coordinate system. The coordinate system moves away from the solid body at a velocity given by, $c'(t)$. In this coordinate system we are looking at the collision of two jets. One comes in from the right (travelling left in Figure 3.2) with a velocity $c'(t)$, and thickness h. The flow from Figure 3.5, from the left (travelling right) into region IV has a velocity $u(c,t) - c'(t)$, where u is given by (3.22). The flow on the

body side of region IV will be of thickness $h+\eta(c,t)$, where η is given by (3.25). This idea is shown in Figure 3.6.

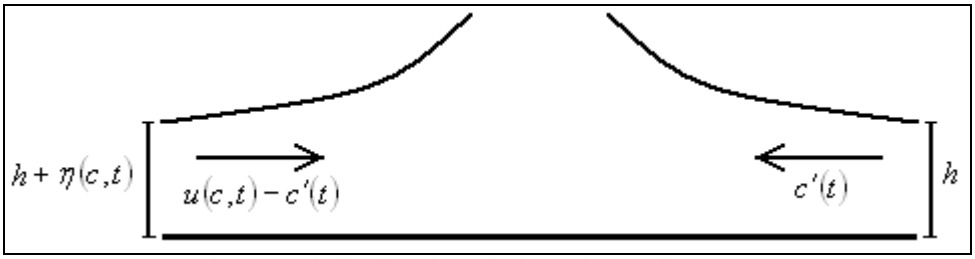

Figure 3.6. The flow in region IV in the moving coordinate system.
We effectively have the steady collision of two opposing jets.

On the free boundary, the fluid domain of (3.25) increases with velocity $c'(t)$. From the dynamical condition (from Bernoulli's equation and since $p=0$ on the free surface) we have that on the free surface the velocity must be constant. On the right-hand side of the free surface in Figure 3.6 this gives us that the velocity of the resulting jet is $c'(t)$. And also,

$$u(c,t)-c'(t)=c'(t). \tag{3.26}$$

Using (3.22) and (3.26) we obtain,

$$\begin{aligned} &\frac{dc}{dt}=\frac{V_0(2L-c)}{2(h-V_0t)}, \\ \Rightarrow\ &\frac{dc}{dt}+\frac{V_0}{2(h-V_0t)}c=\frac{V_0L}{(h-V_0t)}, \end{aligned} \tag{3.27}$$

and we have the initial condition,

$$c(0)=L, \tag{3.28}$$

since $c(t)$ moves away from $x=L$ when $t>0$.

The solution of (3.27) and (3.28) is given by,

$$c(t)=2L-L\sqrt{\frac{h-V_0t}{h}}. \tag{3.29}$$

We can see from (3.29) that c increases from L to $2L$ in the time it takes for the body to reach the bed.

Equation (3.29) gives the velocity of our moving coordinate system as,

$$c'(t)=\frac{V_0L}{2h}\sqrt{\frac{h}{h-V_0t}}. \tag{3.30}$$

Equation (3.30) also gives the velocity of the upward resulting jet (for the reasons stated after Figure 3.6). From (3.25) we have,

$$\eta(c,t) = L^2 \frac{h - V_0 t}{\left(2L - 2L - L\sqrt{\frac{h - V_0 t}{h}}\right)^2} - h = 0\,, \tag{3.31}$$

So, from (3.26) and (3.31), in region IV we have two opposing jets with the same height (h) and equal but opposites velocities $(c'(t))$ resulting in an upward jet with velocity we established as $c'(t)$. Therefore, in order to conserve the amount of fluid, we must have on the grounds of mass (volume) conservation the thickness of this resulting jet is $2h$.

Notice that from Equation (3.30), $c' \to \infty$ as $t \to h/V_0$. Again, we have the solution breaking in this limit. Korobkin [14] notes to correctly describe the flow in this limit we need to take into account the compressibility of the liquid.

3.5. Region V: The splash

In this region we can expect the pressure to be near to atmospheric pressure, and so the fluid moves inertially. The velocity vector in the jet region is made up of components that are both given by $c'(t)$. This is because in section 3.4 we found that the jet's upward velocity is $c'(t)$, and the coordinate system we use moves in the positive x direction with velocity $c'(t)$.

If we now go back to the fixed frame of reference we used for section 3.1-3.3 we have the base of the jet starting at $x = c(0)$ and extending to $x = c'(t)t + c(t)$. The height of the base of the jet is given by $y = c'(t)t$. The velocity field is given by $\mathbf{u} = (c'(t), c'(t))$. We can express the jet parametrically by,

$$x = c'(\tau)(t - \tau) + c(\tau), \quad y = c'(\tau)(t - \tau), \quad \mathbf{u} = (c'(\tau), c'(\tau)), \tag{3.32}$$

where $0 \le \tau \le t$.

We shall attempt to find the shape of the free surface by introducing the two functions $S(y,t)$ and $\xi(y,t)$ such that,

$$x = S(y,t), \tag{3.33}$$

which describes the shape of the left-hand free surface and,

$$x = S(y,t) + h\xi(y,t), \tag{3.34}$$

which describes the right hand free surface.

The kinematic condition (3.6) changes to,

$$\frac{\partial S}{\partial t}+v\frac{\partial S}{\partial y}=u\,, \qquad \text{and,} \tag{3.35a}$$

$$\frac{\partial}{\partial t}\left(S+h\xi\right)+v\frac{\partial}{\partial y}\left(S+h\xi\right)=u\,, \tag{3.35b}$$

on the left hand side of the splash jet and the right hand side respectively.

From (3.32) and (3.35a) we obtain,

$$\frac{\partial S}{\partial t}+c'(\tau)\frac{\partial S}{\partial y}=c'(\tau), \qquad S(0,\tau)=c(\tau),$$

to describe the shape of the left hand side of the jet. This system has the solution,

$$S=c'(\tau)(t-\tau)+c(\tau), \tag{3.36}$$

where we can find τ by, $y=c'(\tau)(t-\tau)$, from (3.32). Using (3.36) along with (3.29) and (3.30), and (3.32) we can explicitly find τ as,

$$\begin{aligned} y=c'(\tau)(t-\tau)&=\frac{V_0L}{2h}\sqrt{\frac{h}{h-V_0t}}(t-\tau),\\ \Rightarrow \tau&=\frac{L^2V_0t-2hy^2-2y\sqrt{y^2h^2-L^2hV_0t+L^2h}}{L^2V_0}, \end{aligned} \tag{3.37}$$

which we can substitute into (3.29), (3.30) and (3.36) to give,

$$\begin{aligned} S&=c'(\tau)(t-\tau)+c(\tau)\\ &=\frac{\left(\begin{array}{l} L^2V_0t-L^2h-hy^2-y\sqrt{h^2y^2-L^2hV_0t+L^2h^2}\\ +2L^2h\sqrt{\dfrac{L^2h+2hy^2-L^2V_0t+2y\sqrt{h^2y^2-L^2hV_0t+L^2h^2}}{L^2h}} \end{array}\right)}{Lh\sqrt{\dfrac{L^2h+2hy^2-L^2V_0t+2y\sqrt{h^2y^2-L^2hV_0t+L^2h^2}}{L^2h}}}. \end{aligned} \tag{3.38}$$

If we introduce Y and T such that $t=hT/V_0$ and $y=LY$, then the equation above and (3.33) give,

$$x=\frac{L\left(T-1-Y^2-Y\sqrt{Y^2-T+1}+2\sqrt{1+2Y^2-T+2Y\sqrt{Y^2-T+1}}\right)}{\sqrt{1+2Y^2-T+2Y\sqrt{Y^2-T+1}}}, \tag{3.39}$$

as the left hand shape of the splash jet at a given time. This is shown in Figure 3.7.

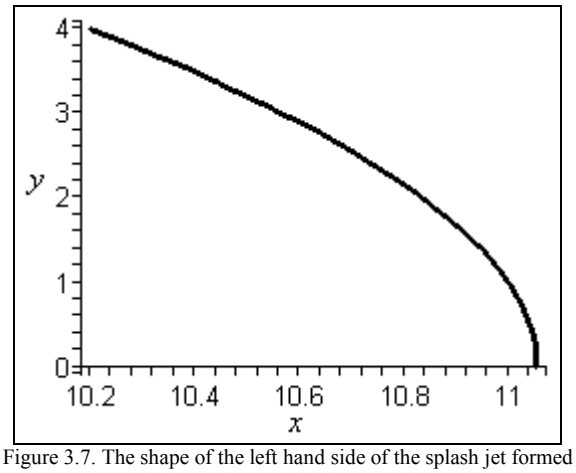

Figure 3.7. The shape of the left hand side of the splash jet formed after 0.2 seconds from when a solid flat, 20m long object enters a fluid of depth 1m at a speed of 1ms^{-1}.

Notice, from Figure 3.7, that the splash jet curves towards the solid object, hence the reason for this portrayal in Figure 3.1. We now wish to find the curve that defines the other side of the jet. Firstly we perform a Taylor expansion on u and v about $x = S(y,t)$ to give,

$$u \approx u\big|_{x=S(y,t)} + \left.\frac{\partial u}{\partial x}\right|_{x=S(y,t)} (x-S) \qquad \text{and,} \qquad v \approx v\big|_{x=S(y,t)} + \left.\frac{\partial v}{\partial x}\right|_{x=S(y,t)} (x-S)$$

$$\Rightarrow u \approx u\big|_{x=S(y,t)} + \left.\frac{\partial u}{\partial x}\right|_{x=S(y,t)} h\xi \qquad \Rightarrow v \approx v\big|_{x=S(y,t)} + \left.\frac{\partial v}{\partial x}\right|_{x=S(y,t)} h\xi$$

from (3.34). Substituting these expansions into (3.35b) gives,

$$\frac{\partial S}{\partial t} + h\frac{\partial \xi}{\partial t} + h\xi\left(v\big|_{x=S(y,t)} + \left.\frac{\partial v}{\partial x}\right|_{x=S(y,t)} \right)\frac{\partial S}{\partial y} + vh\frac{\partial \xi}{\partial t} = u\big|_{x=S(y,t)} + \left.\frac{\partial u}{\partial x}\right|_{x=S(y,t)} h\xi,$$

$$\Rightarrow h\frac{\partial \xi}{\partial t} + \left.\frac{\partial S}{\partial y}\frac{\partial v}{\partial x}\right|_{x=S(y,t)} h\xi + vh\frac{\partial \xi}{\partial t} = +\left.\frac{\partial u}{\partial x}\right|_{x=S(y,t)} h\xi,$$

because of (3.35a). The equation above can be rearranged to give,

$$\frac{1}{\xi}\frac{\partial \xi}{\partial t} + v\frac{1}{\xi}\frac{\partial \xi}{\partial t} = \left[\frac{\partial u}{\partial x} - \frac{\partial S}{\partial y}\frac{\partial v}{\partial x}\right]_{x=S(y,t)},$$

$$\Rightarrow \frac{\partial}{\partial t}(\ln \xi) + v\frac{\partial}{\partial t}(\ln \xi) = -\left[\frac{\partial v}{\partial y} + \frac{\partial S}{\partial y}\frac{\partial u}{\partial y}\right]_{x=S(y,t)}, \qquad (3.40)$$

from (3.2) and (3.33).

From (3.32) and (3.33) we have,

$$\frac{\partial S}{\partial y} = \frac{\partial}{\partial y}\left(c'(\tau)(t-\tau)+c(\tau)\right) = c''(\tau)(t-\tau)\frac{\partial \tau}{\partial y},$$
$$\frac{\partial}{\partial y}(y) = \frac{\partial}{\partial y}\left(c'(\tau)(t-\tau)\right) \Rightarrow 1 = c''(\tau)(t-\tau)\frac{\partial \tau}{\partial y} - c'(\tau)\frac{\partial \tau}{\partial y}$$
$$\Rightarrow c''(\tau)\frac{\partial \tau}{\partial y} = \frac{1}{t-B(\tau)},$$
$$\frac{\partial u}{\partial y} = \frac{\partial v}{\partial y} = c''(\tau)\frac{\partial \tau}{\partial y},$$

where $B(\tau) = \tau + c'(\tau)/c''(\tau)$ since $\tau = \tau(y,t)$. Using the relations above and (3.40) we find,

$$\left[\frac{\partial v}{\partial y} + \frac{\partial S}{\partial y}\frac{\partial u}{\partial y}\right]_{x=S(y,t)} = c''(\tau)\frac{\partial \tau}{\partial y} + (t-\tau)\left[c''(\tau)\frac{\partial \tau}{\partial y}\right]^2$$
$$= \frac{1}{t-B} + \frac{t-\tau}{(t-B)^2} = \frac{2}{t-B} + \frac{B-\tau}{(t-B)^2}.$$

Hence, we need to solve the equation,

$$\frac{\partial}{\partial t}(\ln \xi) + v\frac{\partial}{\partial t}(\ln \xi) = \frac{2}{B-t} + \frac{\tau - B}{(t-B)^2},$$

with the initial condition $\xi(0,t) = 2$, from (3.34) since at the end of section 3.4 we found that the thickness of the base of the jet is 2*h*. The solution to the initial value problem [14] is,

$$\xi(y,t) = \hat{\xi}(t, \tau(y,t)) = 2\left(\frac{\tau - B(\tau)}{t - B(\tau)}\right)^2 \exp\left(\frac{t-\tau}{t-B(\tau)}\right). \tag{3.41}$$

We can use (3.29) to find $B(\tau)$,

$$B(\tau) = \tau + c'(\tau)/c''(\tau) = \tau + \left(\frac{V_0 L}{2h}\left(\frac{h - V_0\tau}{h}\right)^{-1/2}\right) \Big/ \left(\frac{V_0^2 L}{4h^2}\left(\frac{h-V_0\tau}{h}\right)^{-3/2}\right),$$
$$\Rightarrow B(\tau) = \tau + \frac{2h - 2V_0\tau}{V_0} = \frac{2h}{V_0} - \tau,$$

which we can substitute into (3.41) along with (3.37) to obtain,

$$\xi(y,t) = 2A^2 e^{1-A}, \tag{3.42}$$

where,

$$A = 1 + \frac{Y\left(Y + \sqrt{Y^2 - T + 1}\right)}{1 - T + Y\left(Y + \sqrt{Y^2 - T + 1}\right)},$$

and $t = hT/V_0$ and $y = LY$, as before.

Using (3.42) along with (3.34) and (3.38) we can find the shape of the right hand surface of the splash jet. In Figure 3.8 below we have the complete shape of the jet described by (3.42) and also (3.39).

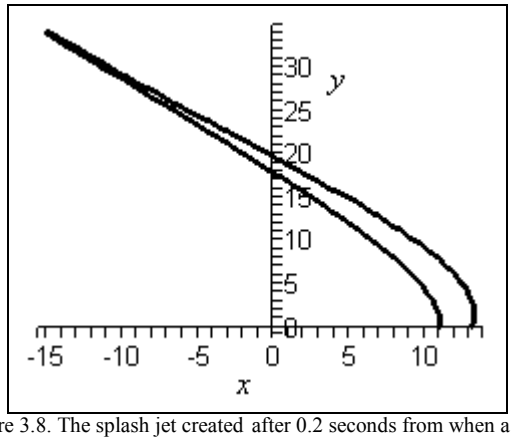

Figure 3.8. The splash jet created after 0.2 seconds from when a solid flat, 20m long object enters a fluid of depth 1m at a speed of $1ms^{-1}$.

Although Figure 3.8 appears to give us a good shape for the jet there are some problems with this solution. Firstly, we were solving the problem for $x > 0$ since we had symmetry in the *y*-axis. From Figure 3.8, we would then end up with two jets crossing the others path. Secondly, the solid object's vertical boundary was in the $x = 10$ line; the jet crosses this line. In a real situation this could suggest two interpretations. If the height of the object were low enough that the jets could overcome it then I would expect the jets to cover the object. If the height of the object was higher than the jet when the jet reached the side of the body, then we would have the impact of a jet on a solid boundary, and a whole new problem we do not have time and space to explore now. We do, however, pick up a similar problem in section 5; a vertical wall accelerating into fluid.

4. Skipping Stones

4.1. The mechanics of skipping stones

On September 14, 2003 Kurt Steiner set a new world record in the category of most ducks and drakes in the game of *Stone-Skipping* [18]. A video clip of this throw can be downloaded from [15]. The record will be revealed in due course, but first we shall try to model the problem to see if we can mathematically estimate the maximum number of skips.

Figure 4.1 below shows the set-up up of the problem we shall be examining.

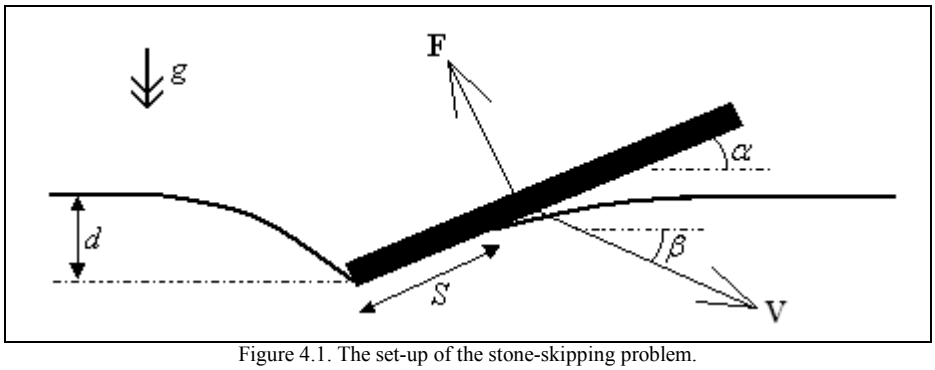

Figure 4.1. The set-up of the stone-skipping problem.

We shall work with a vertical y-axis and a horizontal x-axis in the usual manor, fixing the origin shortly. We shall denote by α the angle at which the plane of the stone is to the positive x-axis. The stone will hit the water at a velocity $\mathbf{V} = (V_x, V_y)$ in the direction given by β. In section 2 we showed that the fluid exerts an impulsive force on an object that hits it from above. We model this by the force **F**, which acts normally to the stone surface. The depth at which the stone penetrates the water is d, and S is the surface area of the stone in contact with the fluid. We have gravity, g, pulling the stone downwards.

The reaction of the water would be expected to take the form [16 and 20],

$$\mathbf{F} = C\rho V^2 S\, f(\alpha, \beta)\mathbf{n},$$

where C is the coefficient of lift, $V^2 = V_x^2 + V_y^2$, and ρ is the density of the fluid. After experimentation, Rosellini *et al*. [19] find the following expression for this force,

$$\mathbf{F} = \tfrac{1}{2}\rho V^2 S \sin(\alpha + \beta)\mathbf{n}. \tag{4.1}$$

Using Newton's second law and some simple trigonometry, from Figure 4.1 and Equation (4.1) we can see that the equations of motion are given by,

$$m\frac{dV_x}{dt} = \frac{1}{2}\rho V^2 S\sin(\alpha+\beta)\sin(\alpha), \qquad \text{and,}$$
$$m\frac{dV_y}{dt} = \frac{1}{2}\rho V^2 S\sin(\alpha+\beta)\cos(\alpha) - mg,$$

when the stone is in contact with the water where *m* is the mass of the stone. Note that in general, *S* is a function of the depth of penetration, which in turn is a function of *t*. When the stone is out of the water we have simply,

$$m\frac{dV_x}{dt} = 0, \qquad \text{and,}$$
$$m\frac{dV_y}{dt} = -mg.$$

If we fix our coordinate axes at the bottom part of the stone in Figure 4.1 at the moment of the first skip, (so the $y=0$ line is the original free surface, and $x=0$ travels vertically through the point of initial contact) then we can express this system as,

$$\frac{dV_x}{dt} = -\frac{\rho K V^2 S\sin(\alpha+\beta)\sin(\alpha)}{2m}, \tag{4.2a}$$
$$\frac{dV_y}{dt} = \frac{\rho K V^2 S\sin(\alpha+\beta)\cos(\alpha)}{2m} - g, \tag{4.2b}$$

where $K = \begin{cases} 1 & \text{if} \quad y \le 0 \\ 0 & \text{if} \quad 0 < y \end{cases}$.

We can also identify $V_y = {}^{dy}\!/_{dt}$, and $V_x = {}^{dx}\!/_{dt}$ [3]. From equations (4.2) we can see that the area of the immersed surface of the stone is an important factor in determining if the stone will be able to rebound off of the fluid surface. Therefore we need to determine the shape of the stone.

I feel it important to note here that despite the apparent simplicity of this type of model so far, Rosellini *et al*. [19] mention that this model agrees well with real experimental data.

4.2. A square stone

We shall first consider a square stone with $\alpha = \text{constant}$. This is obviously a very impossible example in the physical terms, however we start with this shape because of its simpler geometry, enabling me to test the numerical work I will perform shortly. Let the stone have side length *r*, and the depth of the stone will be *h*. We will use a stone such that $\rho_{stone}/\rho_{water} = 2.7$, where ρ is density so we can then compare our work to that of Rosellini *et al*. [19].

Taking $\rho = \rho_{water} = 1$, see the appendix of [2], the mass of our stone will be given by,

$$m = 2.7r^2 h\rho_{water} = 2.7r^2 h\,.$$

The simple geometry of the shape means that the area *S* will be given by,

$$S = \frac{r\,d}{\sin(\alpha)},$$

when the stone is in the water. Since we have fixed our coordinate axes at the base of the stone at first contact, we can identify the depth *d* with the (negative of) coordinate *y* (the stones vertical displacement) when the stone is partly submerged, until the stone is fully submerged. When the stone is fully under water we assume it can no longer rebound, and will sink. Our system of equations then becomes,

$$\frac{dV_x}{dt} = -\frac{\rho K\left(V_x^2 + V_y^2\right) r\, y \sin(\alpha+\beta)\sin(\alpha)}{2m}, \tag{4.3a}$$

$$\frac{dV_y}{dt} = -\frac{\rho K\left(V_x^2 + V_y^2\right) r\, y \sin(\alpha+\beta)\cos(\alpha)}{2m} - g, \tag{4.3b}$$

$$\frac{dx}{dt} = V_x, \tag{4.3c}$$

$$\frac{dy}{dt} = V_y, \tag{4.3d}$$

where the values of *r*, *m*, *K* and ρ were stated earlier.

The system (4.3) is non-linear due to the $\left(V_x^2 + V_y^2\right)$ term. Together with some initial conditions we have enough information to solve (4.3) numerically. This will yield values for V_x, V_y, *x* and *y* at each time step.

We shall firstly consider a stone such that, $r = 0.05\text{m}$ and $h = 0.00275\text{m}$.

I solve this system using the classical Runge-Kutta fourth order scheme [10]. The Maple coding for this numerical procedure is included in A2 of the Appendix. We shall begin with the initial conditions that the stone is thrown at 4ms^{-1} at an angle of 20° with $\alpha = 20°$. I use these conditions because I know from reading [19] we should have some skipping for this stone.

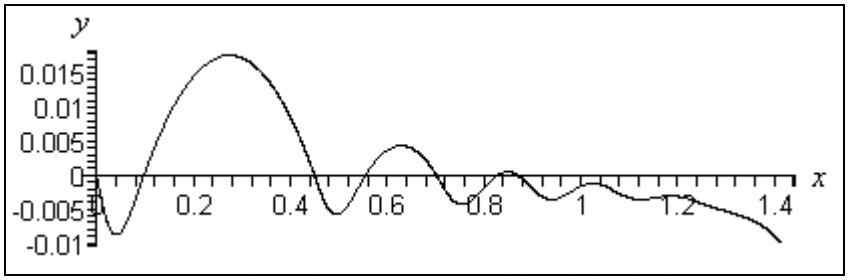

Figure 4.2. The motion of a square stone with a side length of 5cm and depth 2.75mm, thrown at $4ms^{-1}$ and at an angle of $\alpha = 20°$.

We can see from Figure 4.2 that we have a three complete skips, and on the fourth attempt the stone fails to break the water surface and sinks. It is interesting to note how rapid the whole motion is, these three skips and sinking action all occur within the first second.

When playing skipping stones on the beach if the stone is not throw hard enough it simply dives into the water. To check this happens with our system I ran the simulation again, this time changing the initial speed to $1\ ms^{-1}$.

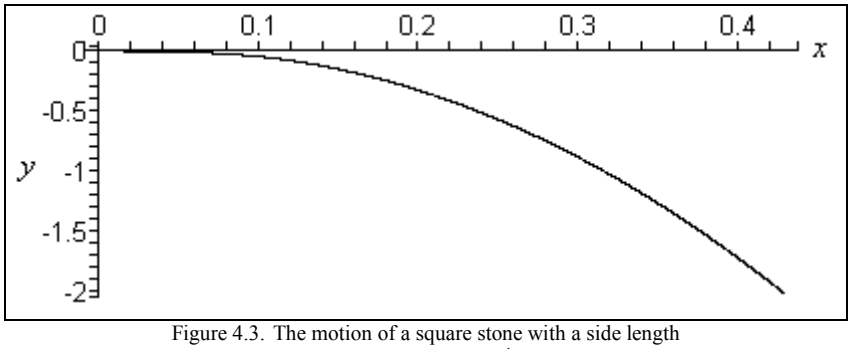

Figure 4.3. The motion of a square stone with a side length of 5cm and depth 2.73mm, thrown at $1ms^{-1}$ and at an angle of 20°.

We can see from Figure 4.3 that the stone sinks if thrown with a low velocity. We shall look more closely at the effects of the parameters in the model when we consider a more realistic situation – a circular stone.

4.3. A circular stone

We shall use a circular stone with a constant value of α. This is feasible since when the stone is given spin it stabilises and so α is approximately constant [3]. If we again use the same ratio for stone and water density that we used for the square stone, then we have

$$m = 2.7\pi r^2 h\ ,$$

for the mass of the stone, where this time r is the radius of the stone and h is the depth.

Since we now have a different shaped stone we have a different expression for *S* (the area of the surface in contact with the water). We can work out the 'wet' area if we consider a circle being dipped in water as shown in Figure 4.4.

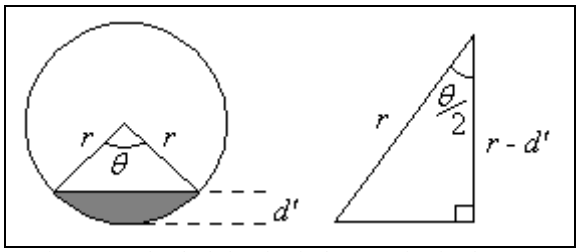

Figure 4.4. The shaded region is the area of a circular stone in contact with the surface of the water.

The length d' in Figure 4.4 is related to *d* in Figure 4.1 by the relation,

$$d' = \frac{d}{\sin(\alpha)}.$$

Using the formula for the area of a segment the 'wet' area in Figure 4.4 is given by,

$$S = \frac{r^2}{2}(\theta - \sin(\theta)). \tag{4.4}$$

Also from Figure 4.4,

$$\theta = 2\cos^{-1}\left(1 - \frac{d'}{r}\right), \quad \text{and,} \quad \tan\left(\frac{\theta}{2}\right) = \frac{\sqrt{r^2 - (r-d')^2}}{r-d'}. \tag{4.5a,b}$$

Using the half angle formulas and (4.5b) we have,

$$\sin(\theta) = \frac{2\sqrt{r^2 - (r-d')^2}}{r-d'} \div \left[1 + \left(\frac{\sqrt{r^2 - (r-d')^2}}{r-d'}\right)^2\right]$$
$$= 2\left(1 - \frac{d'}{r}\right)\sqrt{1 - \left(1 - \frac{d'}{r}\right)^2}.$$

We can then substitute the expression above and (4.5a) into (4.4) to give the wet area of the circular stone as,

$$S = r^2\left[\cos^{-1}\left(1 - \tfrac{d}{r\sin(\alpha)}\right) - \left(1 - \tfrac{d}{r\sin(\alpha)}\right)\sqrt{1 - \left(1 - \tfrac{d}{r\sin(\alpha)}\right)^2}\right]. \tag{4.6}$$

The system we then have to solve is given by equations (4.2) and (4.6) along with, $V_y = {}^{dy}\!/_{dt}$ and $V_x = {}^{dx}\!/_{dt}$, and some initial conditions. Again the numerical scheme is shown in A2 of the Appendix.

We then give our stone the same initial conditions as used to create Figure 4.2. The stone we use has a radius of 2.5cm and a depth of 2.75mm

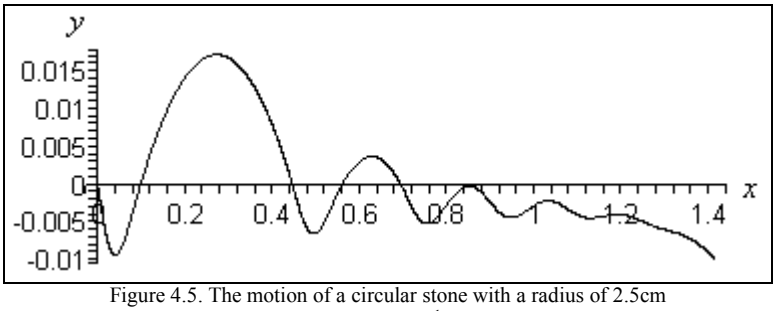

Figure 4.5. The motion of a circular stone with a radius of 2.5cm and depth 2.75mm, thrown at 4ms^{-1} at and an angle of 20°.

Notice from Figures 4.2 and 4.5, we appear to have very similar motion from the square stone and the circular stone. The difference comes in that the circular stone seems to be subjected to a slightly lower force from the water. This is due to the fact that the circular stone has slightly less 'wet' area than the square stone at the same depth.

4.4. Optimising parameters in stone skipping

In Sections 4.2 and 4.3 we have seen how to solve the problem of stone skipping. We may now ask how we can optimise the three parameters α, the initial angle (β), and the initial speed in order to either obtain the maximum amount of skips, or to gain the maximum horizontal range. We continue the stone skipping investigation with the circular stone.

Firstly we shall fix the value of $\beta = 20^\circ$, and vary α and U (which we shall use to denote the velocity at first contact). Figure 2.6 shows the results of varying U for different values of α in order to find a minimum initial velocity needed for the stone to skip.

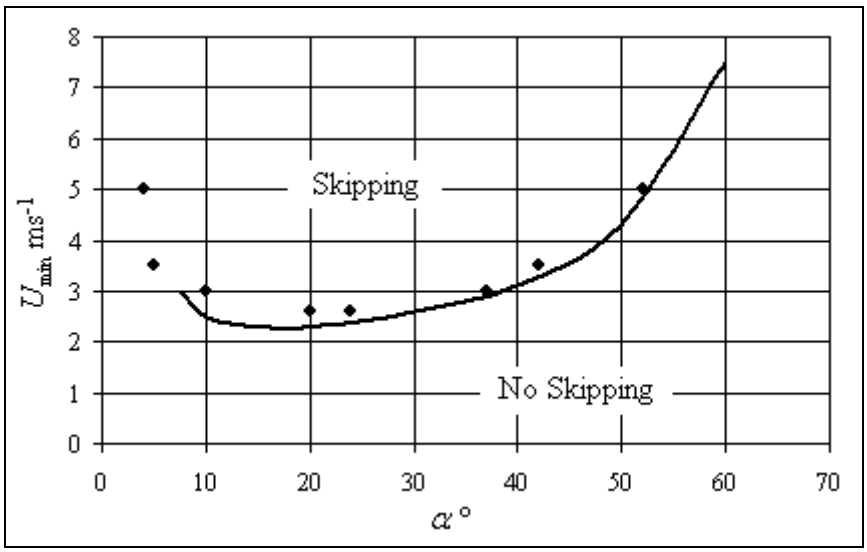

Figure 4.6. The skipping stone domain in the (α, U)-plane, with $\beta = 20°$. The solid line is obtained from the numerical calculations, and the plotted points are from the experiments of Rosellini *et al*. [8].

Figure 4.6 shows agreement with our model and the experimental work by Rosellini *et al*. [19]. They succeed in picking out the boundary line in Figure 4.6. Notice that at a value just before 20° for α we need the lowest initial speed for skipping. From the graph above we can see that $U = 3\text{ms}^{-1}$ is a sufficiently high speed for skipping over a large range of α. (We wish to keep U low so numerical calculation will be quicker in Maple). We shall now fix U at this value and try to find a similar domain in the parameters α and β. This is seen in Figure 4.7.

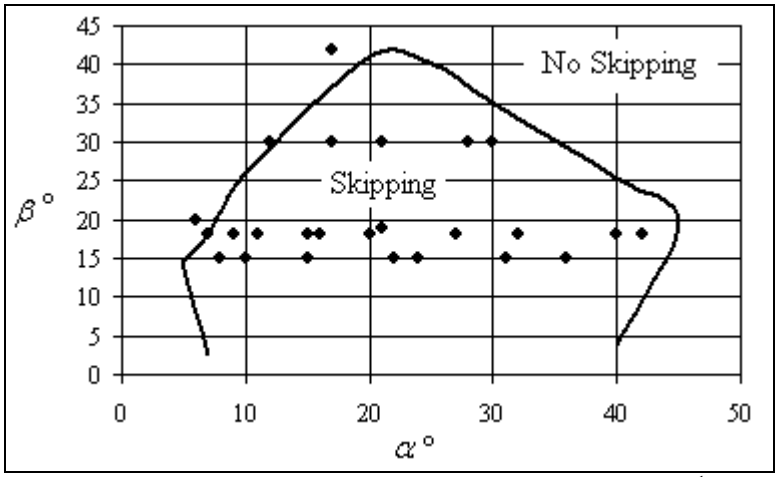

Figure 4.7. The skipping stone domain in the (α, β)-plane, with $U = 3\text{ms}^{-1}$. The solid line is obtained from the model described by Equations 4.2 and 4.6, and the plotted points are from the experiments from [8].

From Figure 4.7 we can see the domain in which we can change α and β simultaneously in order to have the stone rebounding off the water surface. Again we appear to have similar results from the experiments of Rosellini *et al.* [19]. From the diagram a value of 20° for α appears to give us a good range in which we can vary β. We can also see that values of β between 15° and 20° give a good range of α for skipping.

Since a value of near 20° for α gave us the biggest range for U and β to achieve skipping we will use this as our value for α.

I mentioned in the introduction that the idea of rebounding cannon ball was used in the battle of Trafalgar. Miloh and Shukron [17] note that the optimum angle to maximise the range of cannon balls after bouncing (analogous to our β) is $18^{\circ}/\sqrt{\sigma}$, where σ is the density ratio we set earlier at 2.7. The authors concede that they cannot find a source for this angle.

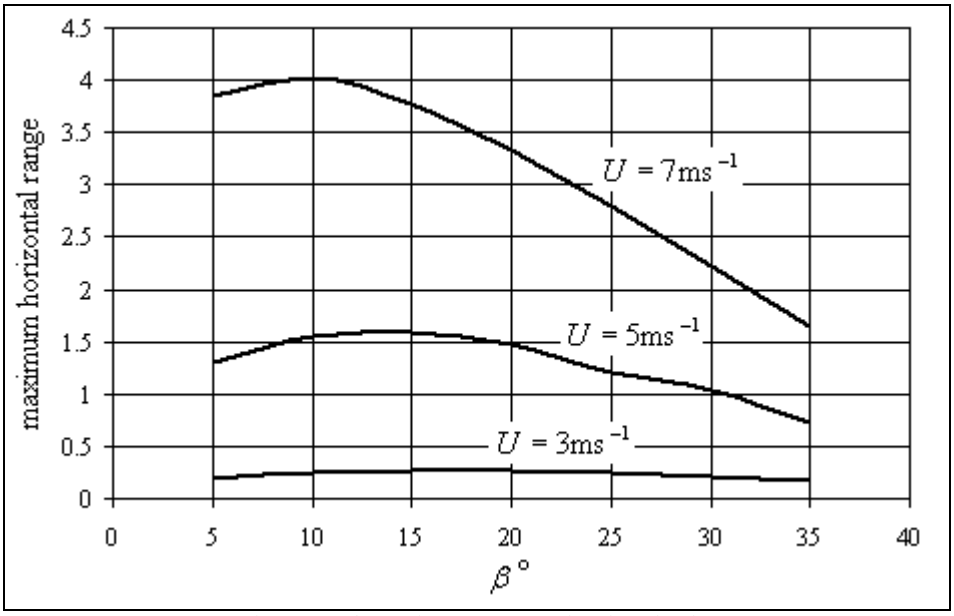

Figure 4.8. The maximum range as a function of β, for different values of U. Here $\alpha = 20°$.

From Figure 4.8 we can see that there does appear to be an optimum angle for β for each value of U in order to maximise horizontal range. This value appears to be different for different values of U. Using the formula from [17] we would expect the maximum range to be achieved when $\beta \approx 11^{\circ}$. This appears to be true for the initial velocity $U = 7\text{ms}^{-1}$.

The idea of maximum range brings us back to the world record I opened this chapter with, that of the highest number of skips. Figure 4.9 below shows the total number of skips as a function of U for different values of β.

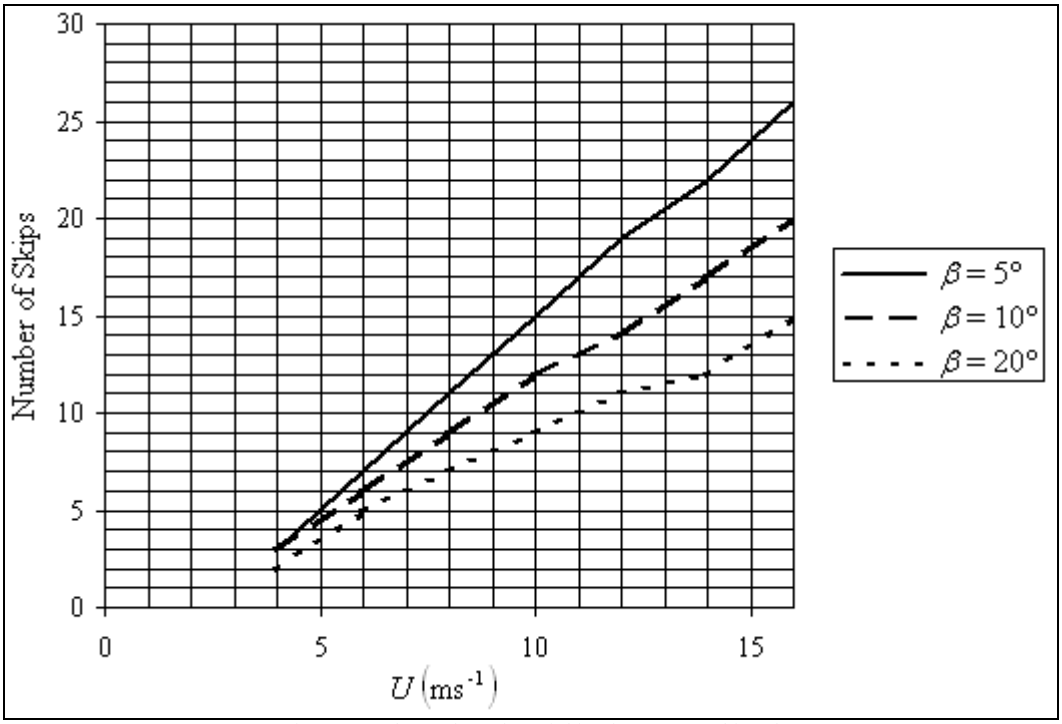

Figure 4.9. The total number of skips for a stone achieved when thrown with different initial speeds, for different values of β.

Figure 4.9 appears to suggest that it is possible to obtain more skips when the stone is thrown with an almost flat trajectory. It appears that the number of skips achieved is a linear function of U, and the gradient increases with decreasing β.

Interestingly, if we vary both α and β simultaneously, we can obtain a high number of skips when both α and β are both small angles. For example if we set $\alpha = 8°$ and $\beta = 5°$, and let $U = 12\text{ms}^{-1}$ (a typical value from a human throw) we obtain 38 skips. This is the previous record beaten by Kurt Steiner when he achieved 40 skips [18]. Is this record beatable? The work we have performed appears to suggest it is. Since the maximum number of skips is a linear function of U (the initial velocity), it is simply a matter of throwing the stone faster.

5. A Horizontally Accelerating Vertical Plate

5.1. Finding the free surface profile

We begin this chapter with a summary of the work by King and Needham [11] on a vertical plate accelerating horizontally into water initially at rest. Many of the diagrams and equations that follow may be the same or similar to those found in that paper. King and Needham [11] find the free surface profile shown in Figure 5.1, but do not go on to look at the pressure distribution in the fluid. We extend their work in order to study this pressure distribution. In order that readers can follow this section of the report in conjunction with [11] the notation is consistent.

Figure 5.1 shows the set-up of the problem. We have a plate accelerating (uniformly) from left to right with constant acceleration $a > 0$. The fluid is initially at rest at a height *h* above the fluid bed.

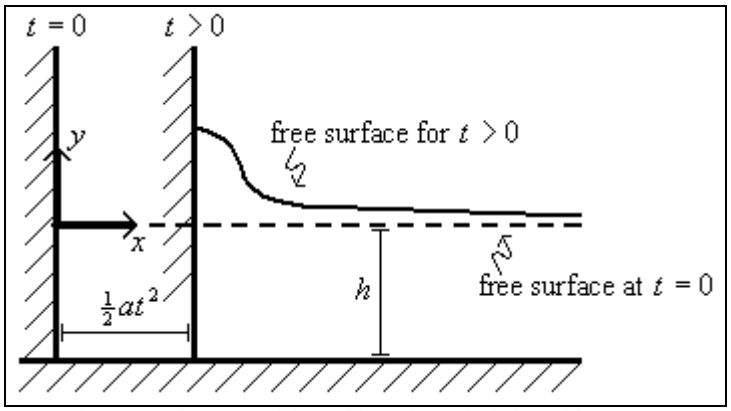

Figure 5.1. The set-up of the problem of a vertical plate with constant horizontal acceleration moving into a liquid initially at rest.

If we let $t = 0$ to be when the system is at rest, the distance the plate travels is given by $\frac{1}{2}at^2$. We begin by non-dimensionalising the problem using,

$$\mathbf{x}' = \frac{\mathbf{x}}{h}, \quad \mathbf{v}' = \frac{\mathbf{v}}{(gh)^{1/2}}, \quad t' = t\left(\frac{g}{h}\right)^{1/2}, \quad p' = \frac{p}{\rho gh}, \tag{5.1}$$

where $\mathbf{x} = (x, y)$ and $\mathbf{v} = (u, v)$ are the usual position and velocity vectors, *t* and *p* are time and pressure respectively. The fluid density, ρ, and gravity, *g*, are assumed to be constant. We also introduce the parameter $\sigma = a/2g$ so $u' = 2\sigma t$ on the moving plate. Since for the remaining part of the chapter we shall work on the non-dimensionalised problem, we will omit the primes.

Using Euler's equation of motion for a fluid the problem is represented by,

$$u_x + v_y = 0,$$
$$u_t + uu_x + vu_y = -p_x,$$
$$v_t + uv_x + vv_y = -p_y - 1.$$

If the free surface is denoted by $y = \eta(x,t)$ then we have $\eta(x,0) = u(x,y,0) = v(x,y,0) = 0$ as initial conditions. On $y = \eta(x,t)$ we have $v = \eta_t + x_t\eta_x$ on the free surface, as well as the condition $p = 0$. On the horizontal bed of Figure 5.1 we have $v(x,-1,t) = 0$, and as $x \to \infty$ we have $u, v \to 0$. Also if $h \to \infty$ we shall model the pressure such that $p \sim -y$ as $x \to \infty$.

King and Needham solve this problem for a small time solution. The mathematics is lengthy and we only require the solution for this report and so we only summarise the main findings here. (Suffice to say the solutions are derived in [11]). The solution to the problem above is,

$$p = -y - \frac{16}{\pi^2}\sum_{n=0}^{\infty}\frac{e^{-\left(n+\frac{1}{2}\right)\pi x}}{(2n+1)^2}\sin\left(\left(n+\tfrac{1}{2}\right)\pi y\right) + \mathrm{O}(t), \text{ and,} \tag{5.2}$$

$$\eta = \frac{2\sigma}{\pi}t^2\ln\left[\coth\left(\pi x/4\right)\right] + \mathrm{O}\left(t^3\right). \tag{5.3}$$

Equations (5.2) and (5.3) give an outer solution of the free surface profile and pressure distribution. The problem comes in that there is a singularity in η as $x \to 0$. This means we need to look more closely at the intersection of the free surface and the vertical wall using approximations of a higher order. King and Needham [11] call this region the "inner region". They use the techniques of asymptotic expansions and Mellin transformations to arrive at a solution of the form,

$$p = t^2\ln^2(t)p_1 + t^2\ln(t)p_2 + o\left(t^2\ln(t)\right), \qquad \text{and,} \tag{5.4}$$
$$\eta = -t^2\ln(t)\eta_1 - t^2\eta_2 + o\left(t^2\right), \tag{5.5}$$

where,

$$p_1 = \frac{8\sigma}{\pi}\left(\frac{y}{t^2\ln(t)} + \frac{4\sigma}{\pi}\right), \qquad \eta_1 = \frac{4\sigma}{\pi}, \tag{5.6}$$

and,

$$p_2 = p_0 + 3\phi - 2X\phi_x + 2\left[\frac{y}{t^2\ln(t)}\frac{4\sigma}{\pi}\right]\phi_y, \tag{5.7}$$

$$\eta_2 = \frac{2\sigma}{\pi}\left[\ln(x) + \lambda\right] + \tfrac{1}{2}\sigma\pi^{\frac{1}{2}}\frac{1}{2\pi i}\int_{c-i\infty}^{c+i\infty}\frac{(2\sigma/\pi X)^p}{p(1+p)\sin\left(\frac{1}{2}\pi p\right)\Gamma\left(p+\frac{3}{2}\right)}dp, \tag{5.8}$$

where, $0 < c < 2$, and,

$$\lambda = \ln\left[-\ln(t)\right] - \ln(4/\pi), \qquad X = -\frac{x}{t^2 \ln(t)}, \qquad \text{and}$$

$$\phi = \frac{16\sigma^2}{6\pi^2}\ln\left(1+r^2\right) - \frac{4\sigma}{\pi}\left\{r\sin(\theta)\ln(r) + r\theta\cos(\theta) + (\lambda+1)r\sin(\theta)\right\}$$

where we have used standard polar coordinates to express ϕ, and the constant p_0 can be evaluated from the surface pressure.

King and Needham note that after application of the residue theorem the integral,

$$\eta^* = -\frac{1}{4}\frac{1}{2\pi i}\int_{c-i\infty}^{c+i\infty} \frac{(2\sigma/\pi X)^p}{p(1+p)\sin\left(\frac{1}{2}\pi p\right)\Gamma\left(p+\frac{3}{2}\right)}dp\,,$$

can be written as,

$$\eta^* = -\frac{1}{2\pi}\sum_{n=1}^{\infty} \frac{(-1)^n (2\sigma/\pi X)^{2n}}{2n(2n+1)\Gamma\left(2n+\frac{3}{2}\right)}. \tag{5.9}$$

A graph of this function is shown below.

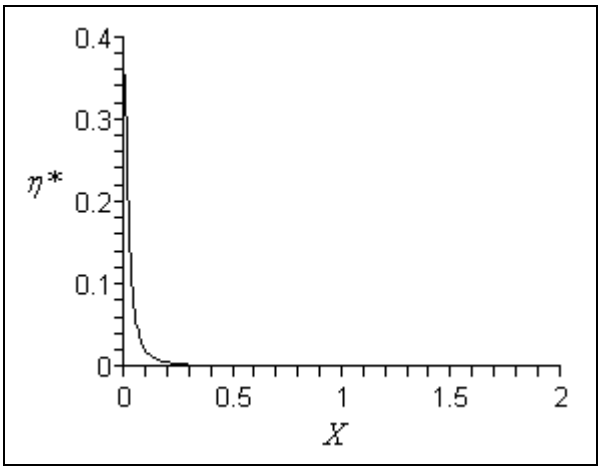

Figure 5.2. The function η^* with $\sigma = 0.25$.

As we can see from Figure 5.2, we still have a singularity in (5.8) as $x \to 0$. We therefore need to look at (5.8) more closely for smaller values of *x*. As $x \to 0$ Equation (5.8) becomes,

$$\eta_2(X) \approx \frac{2\sigma}{\pi}\left\{\ln\left[-\ln(t)\right] - \ln\left(\frac{4}{\pi}\right) + \ln\left(\frac{2\sigma}{\pi}\right) - 1 - \frac{\Gamma'\left(\frac{3}{2}\right)}{\Gamma\left(\frac{3}{2}\right)} + \frac{\pi^2 X}{8\sigma}\right\}. \tag{5.10}$$

Equation (5.10) shows that the free surface leaves the wall linearly. Substituting (5.6) and (5.10) into (5.5) when $x = X = 0$ gives,

$$\eta = -\frac{4\sigma}{\pi}t^2\ln(t) - \frac{2\sigma t^2}{\pi}\left\{\ln\left[-\ln(t)\right] - \ln\left(\frac{4}{\pi}\right) + \ln\left(\frac{2\sigma}{\pi}\right) - 1 - \frac{\Gamma'\left(\frac{3}{2}\right)}{\Gamma\left(\frac{3}{2}\right)}\right\}, \tag{5.11}$$

as the height of the free surface at the point of contact with the moving plate.

5.2. Graphing solutions to the problem

From the last section we have arrived at some expressions for the shape of the free surface in Figure 5.1, as well as expressions for the pressure distribution in the fluid. Let us now see what these solutions look like.

Firstly we found Equation (5.3) gave a good approximation to the shape of the free surface. Figure 5.3 shows the profile this equation represents.

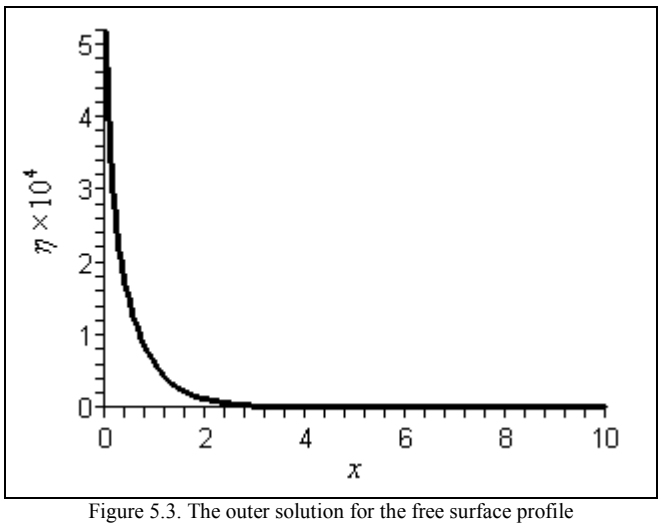

Figure 5.3. The outer solution for the free surface profile as given by Equation (5.3), with $\sigma = 0.25$ at $t = 0.03$.

Recall that is was an outer solution valid for larger values of x. We can see η is logarithmically singular as $x \to 0$. This singularity forces a closer analysis of this inner region. From Equation (5.10) we have the free surface leaving the wall in a linear manner at a height given by (5.11). The free surface then decays as given by Equations (5.5), (5.6) and (5.8). To create the picture of this below, the integral in Equation (5.8) has been calculated using Equation (5.9).

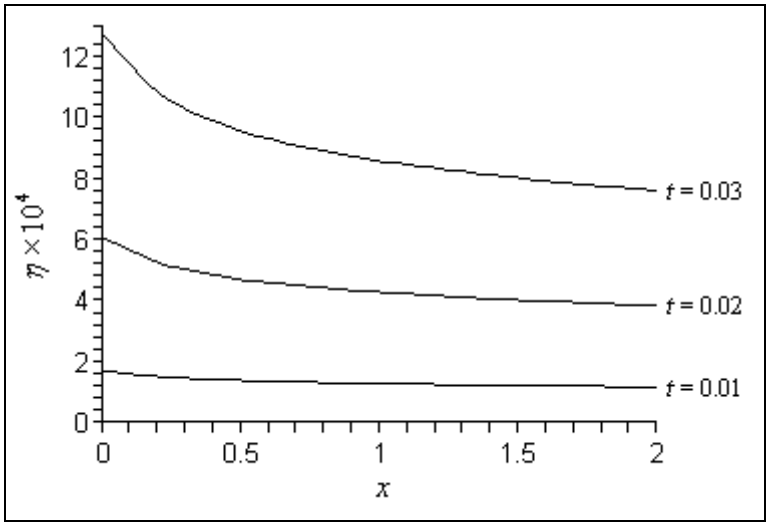

Figure 5.4. The free surface profile for the inner solution, with $\sigma = 0.25$.

Figure 5.4 has been created at three different time steps. We can see that the gradient increases as time progresses, as well as the height of the free surface and vertical wall intersection point.

We also calculated the pressure distribution for the fluid away from the intersection in our fluid domain. This was given by Equation (5.2), and is seen below in Figure 5.5.

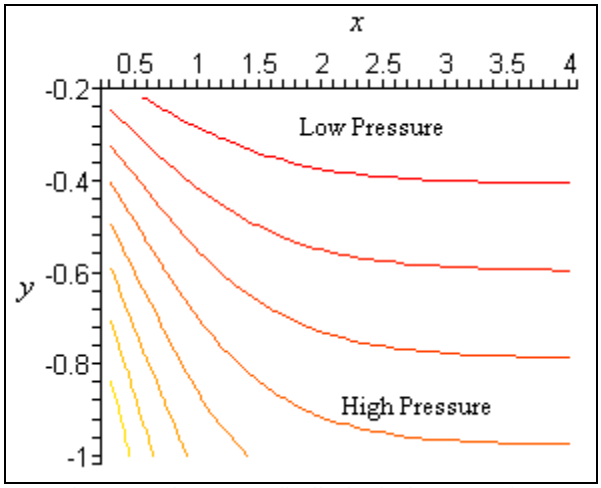

Figure 5.5. The pressure distribution in the outer region.
Lines in the plotting area connect points of constant pressure.

From Figure 5.5 we appear to have the highest pressure point in the corner between the vertical wall and fluid bed. This build-up of pressure is why the free surface is pushed up the wall. Since the maximum pressure (away from the free surface and vertical wall intersection) is at this corner between the two solid walls in Figure 5.1, we can see the example we are studying has a completely different pressure distribution from that of the deep-water case, where the vertical wall does not touch the fluid bed.

More interesting is the pressure distribution in the inner region given by equation (5.4), shown in Figure 5.6 below.

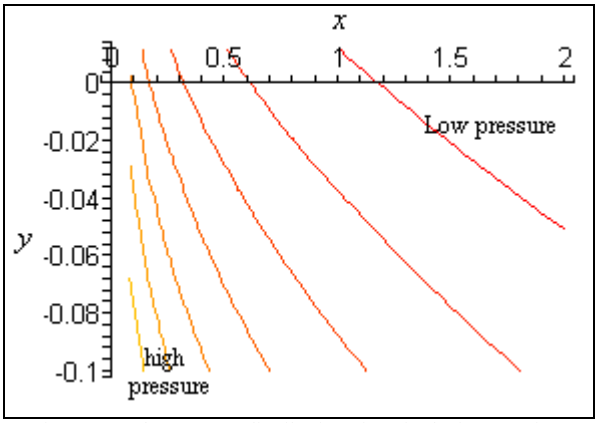

Figure 5.6. The pressure distribution given in the inner region.

Figure 5.6 appears to show us the same type of behaviour we have in the outer region that we saw in Figure 5.5. When engineers build structures such as seawalls (which is of course the same situation we have been modelling from the view point of sitting on

the vertical plate) they model the pressure on the wall with a trapezoidal distribution (see for example pages 134 and 135 of [6]). This would lead us to expect a local maximum on the plate near $y = 0$. Figure 5.7 shows an enlargement of this region.

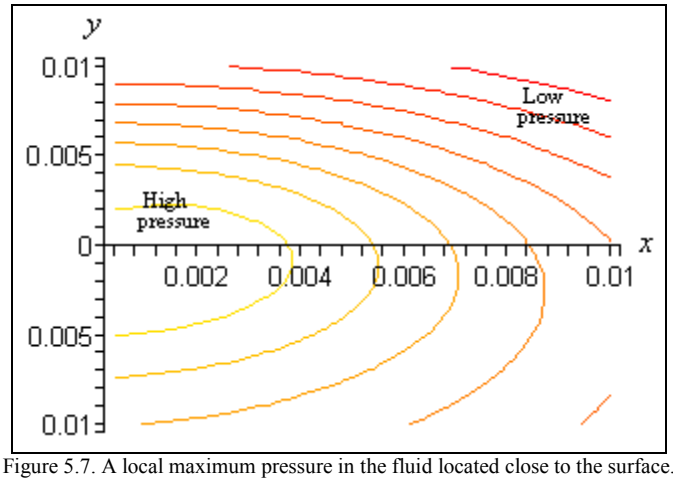

Figure 5.7. A local maximum pressure in the fluid located close to the surface.

Figure 5.7 shows the result we would have expected from the engineers empirical laws that suggest a high-pressure region in the area of the original free surface and wall intersection. Figure 5.8 highlights what we have just seen. It shows the pressure distribution along the plate. There are no values on the axes due to computing difficulties. The shape of the pressure distribution is more interesting than the actual values of pressure. Figure 5.8 extends only about 40% of the distance down the wall since the pressure grows so greatly that the local maximum near the surface cannot be seen in the Maple graphics.

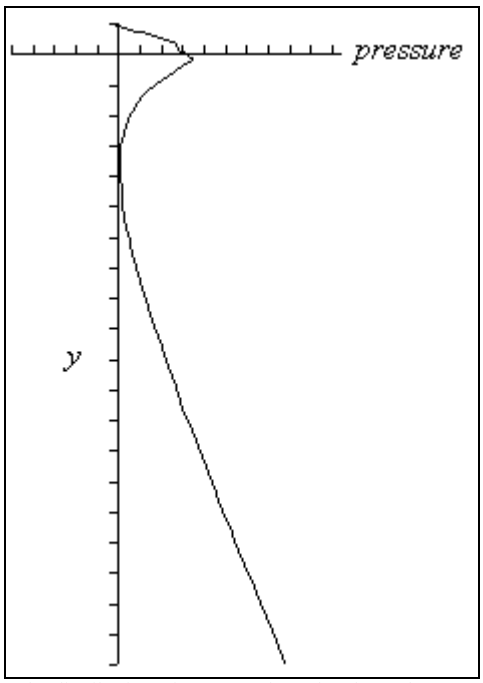

Figure 5.8. The distribution of pressure along the plate. The *pressure*-axis is in the same place as the *x*-axis in Figure 5.7. Here $t = 0.03$ as in Figure 5.7.

The presence of a local maximum in pressure at the plate near $y = 0$ is associated with the high pressure gradient at the free surface, which in turn is associated with the

large upward acceleration of the free surface. The ratio of the local maximum near the free surface and the global maximum in pressure appears to change with time. For example, when $t = 0.01$ this ratio was of the order 10^{-2}, where as at $t = 0.05$ this ratio had grown to be of order 10^{-1}.

6. Conclusion

During this project I have tried to outline what I consider some of the more interesting topics in the impact of a solid body with a fluid surface. We began by considering a solid object entering fluid from above and showed that there is an associated impulsive force exerted on the body from the fluid at the moment of impact. We also saw that there was a singularity in the mathematics for the free surface profile at the intersection with the solid as the body entered the fluid. Clearly in the physical world we could not have singular behaviour for a fluid free surface and so in section 3 we took a closer look at this region to examine the splash in more detail.

Picking up the work of Korobkin [14] in section 3 we examined the splash jet created from a solid box-like object impacting on a fluid with a shallow depth. By dividing the fluid domain into separate regions we were able to show, to first order, the splash jet curved in towards the solid body. The jet moved away from the body with a velocity dependent on the speed and size of the solid body and the depth of the fluid. We also saw that, depending on the height of the solid body, the jet would either pass over the object or impact the side of it.

In section 4 we took the idea of the impulsive force from the fluid on an impacting solid body to look at the favourite seaside game, skipping stones. We first set up the equations of motion and showed, with numerical calculations, that it is possible to make an idealised square stone skip along the water surface. We then moved on to a more realistic circular flat stone, and managed to find domains for the parameters (stone angle, initial velocity and initial direction) in which skipping could occur. The domains we found concurred with experimental work done by Rosellini *et al*. [19]. We also found that the maximum number of skips was a linear function of the initial throw speed. Therefore, impressive though it is, Kurt Steiner's world record throw of 40 skips is beatable.

In the introduction to the project we mentioned that shipping provides some good physical examples of the work we have covered. This led me to the question of the jet created as a solid wall travels vertically through a fluid, for example the front of a ship. We began section 5 with a review of the work by King and Needham [11] that gave us the free surface profile. We then extended this work to look more closely at the pressure distribution in the fluid created from the moving wall. In particular we looked at the pressure distribution along the plate and discovered the mathematical analysis we carried out agreed closely with the empirical laws used by engineers (described in [6]). We found the existence of a high-pressure region at a level just below the free surface on the vertical wall.

All the work presented here is of relevance in many areas. Principally in important areas such as shipping and sea defence structures, but also recreations, such as stone skipping. During this project I have discovered how vast a subject water impact problems is (see for example [12] for some related problems and an extensive list of

related literature) and hope that the few examples I have chosen to highlight in the dissertation scratches the surface of some of these topics.

Appendix

A1. Finding the differential equation for $F(\xi)$

We are looking for a solution of,

$$\frac{\partial^2\psi}{\partial x^2}+\frac{\partial^2\psi}{\partial y^2}-\frac{1}{y}\frac{\partial\psi}{\partial y}=0\ , \tag{A1}$$

in the form,

$$\psi = F(\xi)\sin^2(\eta)\ . \tag{A2}$$

From Equations (2.11) we had,

$$\frac{\partial}{\partial x}\equiv\frac{\cosh(\xi)\cos(\eta)}{\left(a^2-b^2\right)^{1/2}\left\{\sinh^2(\xi)+\cos^2(\eta)\right\}}\frac{\partial}{\partial\xi}-\frac{\sinh(\xi)\sin(\eta)}{\left(a^2-b^2\right)^{1/2}\left\{\sinh^2(\xi)+\cos^2(\eta)\right\}}\frac{\partial}{\partial\eta}\ , \tag{A3}$$

$$\frac{\partial}{\partial y}\equiv\frac{\sinh(\xi)\sin(\eta)}{\left(a^2-b^2\right)^{1/2}\left\{\sinh^2(\xi)+\cos^2(\eta)\right\}}\frac{\partial}{\partial\xi}+\frac{\cosh(\xi)\cos(\eta)}{\left(a^2-b^2\right)^{1/2}\left\{\sinh^2(\xi)+\cos^2(\eta)\right\}}\frac{\partial}{\partial\eta}\ . \tag{A4}$$

To simplify the equations that will follow we shall introduce,

$$A(\xi,\eta)=\frac{\sinh(\xi)\sin(\eta)}{\left(a^2-b^2\right)^{1/2}\left\{\sinh^2(\xi)+\cos^2(\eta)\right\}},\qquad \text{and,} \tag{A5}$$

$$B(\xi,\eta)=\frac{\cosh(\xi)\cos(\eta)}{\left(a^2-b^2\right)^{1/2}\left\{\sinh^2(\xi)+\cos^2(\eta)\right\}}. \tag{A6}$$

From (A3) and (A2) we have,

$$\frac{\partial\psi}{\partial y}=A\psi_\xi+B\psi_\eta\ ,$$

$$\frac{\partial\psi}{\partial x}=B\psi_\xi-A\psi_\eta\ ,$$

$$\frac{\partial^2\psi}{\partial y^2}=A^2\psi_{\xi\xi}+AA_\xi\psi_\xi+2AB\psi_{\xi\eta}+AB_\xi\psi_\eta+A_\eta B\psi_\xi+B^2\psi_{\eta\eta}+BB_\eta\psi_\eta\ ,$$

$$\frac{\partial^2\psi}{\partial x^2} = B^2\psi_{\xi\xi} + BB_\xi\psi_\xi - 2AB\psi_{\xi\eta} - A_\xi B\psi_\eta - AB_\eta\psi_\xi + A^2\psi_{\eta\eta} + AA_\eta\psi_\eta .$$

If we now substitute the four equations above into (A1) and divide through by $\left(A^2 + B^2\right)$ we obtain,

$$\psi_{\xi\xi} + \psi_{\eta\eta} + \left[\frac{AA_\xi + BA_\eta + BB_\xi - AB_\eta - A/y}{A^2 + B^2}\right]\psi_\xi + \left[\frac{AB_\xi + BB_\eta - BA_\xi + AA_\eta - B/y}{A^2 + B^2}\right]\psi_\eta = 0 . \qquad \text{(A7)}$$

We shall introduce the simplifications,

$$C = \frac{AA_\xi + BA_\eta + BB_\xi - AB_\eta - A/y}{A^2 + B^2}, \quad \text{and,} \quad D = \frac{AB_\xi + BB_\eta - BA_\xi + AA_\eta - B/y}{A^2 + B^2}.$$

From (A2) we have,

$$\psi_\xi = F'\sin^2(\eta),$$

$$\psi_\eta = 2F\sin(\eta)\cos(\eta),$$

$$\psi_{\xi\xi} = F''\sin^2(\eta), \qquad \text{and,}$$

$$\psi_{\eta\eta} = 2F\cos^2(\eta) - 2F\sin^2(\eta) = 2F\cos(2\eta),$$

which we can substitute into (A7) and divide through by $\sin^2(\eta)$ to obtain,

$$F'' + CF' + \frac{2D\sin(\eta)\cos(\eta) + 2\cos(2\eta)}{\sin^2(\eta)}F = 0 . \qquad \text{(A8)}$$

From (A5) we have,

$$A_\xi = \frac{\left(a^2 - b^2\right)^{1/2}\left\{\sinh^2(\xi) + \cos^2(\eta)\right\}\cosh(\xi)\sin(\eta) - 2\left(a^2 - b^2\right)^{1/2}\sinh^2(\xi)\cosh(\xi)\sin(\eta)}{\left(a^2 - b^2\right)\left\{\sinh^2(\xi) + \cos^2(\eta)\right\}^2}$$

$$= \frac{\cosh(\xi)\sin(\eta)\left[\cos^2(\eta) - \sinh^2(\xi)\right]}{\left(a^2 - b^2\right)^{1/2}\left\{\sinh^2(\xi) + \cos^2(\eta)\right\}^2}, \qquad \text{and,} \qquad \text{(A9)}$$

$$A_\eta = \frac{\left(a^2 - b^2\right)^{1/2}\left\{\sinh^2(\xi) + \cos^2(\eta)\right\}\sinh(\xi)\cos(\eta) + 2\left(a^2 - b^2\right)^{1/2}\cos(\eta)\sin^2(\eta)\sinh(\xi)}{\left(a^2 - b^2\right)\left\{\sinh^2(\xi) + \cos^2(\eta)\right\}^2}$$

$$= \frac{\sinh(\xi)\cos(\eta)\left[\cosh^2(\xi)+\sin^2(\eta)\right]}{\left(a^2-b^2\right)^{1/2}\left\{\sinh^2(\xi)+\cos^2(\eta)\right\}^2}. \qquad \text{(A10)}$$

From (A6) we have,

$$B_\xi = \frac{\left(a^2-b^2\right)^{1/2}\left\{\sinh^2(\xi)+\cos^2(\eta)\right\}\sinh(\xi)\cos(\eta) - 2\left(a^2-b^2\right)^{1/2}\cosh^2(\xi)\sinh(\xi)\cos(\eta)}{\left(a^2-b^2\right)\left\{\sinh^2(\xi)+\cos^2(\eta)\right\}^2}$$

$$= -\frac{\sinh(\xi)\cos(\eta)\left[\sin^2(\eta)+\cosh^2(\xi)\right]}{\left(a^2-b^2\right)^{1/2}\left\{\sinh^2(\xi)+\cos^2(\eta)\right\}^2}, \qquad \text{and,} \qquad \text{(A11)}$$

$$B_\eta = \frac{2\left(a^2-b^2\right)^{1/2}\sin(\eta)\cos^2(\eta)\cosh(\xi) - \left(a^2-b^2\right)^{1/2}\left\{\sinh^2(\xi)+\cos^2(\eta)\right\}\cosh(\xi)\sin(\eta)}{\left(a^2-b^2\right)\left\{\sinh^2(\xi)+\cos^2(\eta)\right\}^2}$$

$$= \frac{\cosh(\xi)\sin(\eta)\left[\cos^2(\eta)-\sinh^2(\xi)\right]}{\left(a^2-b^2\right)^{1/2}\left\{\sinh^2(\xi)+\cos^2(\eta)\right\}^2}. \qquad \text{(A12)}$$

From (A5) and (A6) we also have,

$$A^2+B^2 = \frac{\sinh^2(\xi)\sin^2(\eta)+\cosh^2(\xi)\cos^2(\eta)}{\left(a^2-b^2\right)\left\{\sinh^2(\xi)+\cos^2(\eta)\right\}^2}$$

$$= \frac{1}{\left(a^2-b^2\right)\left\{\sinh^2(\xi)+\cos^2(\eta)\right\}}. \qquad \text{(A13)}$$

Using (A5) and (A6) with the equations given by (A9)-(A12) we have the relations,

$$AA_\xi = \frac{\sinh(\xi)\cosh(\xi)\sin^2(\eta)\left[\cos^2(\eta)-\sinh^2(\xi)\right]}{\left(a^2-b^2\right)\left\{\sinh^2(\xi)+\cos^2(\eta)\right\}^3},$$

$$BA_\xi = \frac{\cosh^2(\xi)\cos(\eta)\sin(\eta)\left[\cos^2(\eta)-\sinh^2(\xi)\right]}{\left(a^2-b^2\right)\left\{\sinh^2(\xi)+\cos^2(\eta)\right\}^3},$$

$$AA_\eta = \frac{\sinh^2(\xi)\sin(\eta)\cos(\eta)\left[\cosh^2(\xi)+\sin^2(\eta)\right]}{\left(a^2-b^2\right)\left\{\sinh^2(\xi)+\cos^2(\eta)\right\}^3},$$

$$BA_\eta = \frac{\sinh(\xi)\cosh(\xi)\cos^2(\eta)\left[\cosh^2(\xi)+\sin^2(\eta)\right]}{\left(a^2-b^2\right)\left\{\sinh^2(\xi)+\cos^2(\eta)\right\}^3},$$

$$AB_\xi = -\frac{\sinh^2(\xi)\cos(\eta)\sin(\eta)\left[\sin^2(\eta)+\cosh^2(\xi)\right]}{\left(a^2-b^2\right)\left\{\sinh^2(\xi)+\cos^2(\eta)\right\}^3},$$

$$BB_{\xi} = -\frac{\sinh(\xi)\cosh(\xi)\cos^2(\eta)\left[\sin^2(\eta)+\cosh^2(\xi)\right]}{\left(a^2-b^2\right)\left\{\sinh^2(\xi)+\cos^2(\eta)\right\}^3},$$

$$AB_{\eta} = \frac{\sinh(\xi)\cosh(\xi)\sin^2(\eta)\left[\cos^2(\eta)-\sinh^2(\xi)\right]}{\left(a^2-b^2\right)\left\{\sinh^2(\xi)+\cos^2(\eta)\right\}^3}, \qquad \text{and,}$$

$$BB_{\eta} = \frac{\cosh^2(\xi)\sin(\eta)\cos(\eta)\left[\cos^2(\eta)-\sinh^2(\xi)\right]}{\left(a^2-b^2\right)\left\{\sinh^2(\xi)+\cos^2(\eta)\right\}^3}.$$

Using (A13) along with the relations above we obtain,

$$\frac{AA_{\xi}}{A^2+B^2} = \frac{\sinh(\xi)\cosh(\xi)\sin(\eta)\cos(\eta)\left[\cos^2(\eta)-\sinh^2(\xi)\right]}{\left\{\sinh^2(\xi)+\cos^2(\eta)\right\}^2}, \tag{A14}$$

$$\frac{BA_{\xi}}{A^2+B^2} = \frac{\cosh^2(\xi)\cos(\eta)\sin(\eta)\left[\cos^2(\eta)-\sinh^2(\xi)\right]}{\left\{\sinh^2(\xi)+\cos^2(\eta)\right\}^2}, \tag{A15}$$

$$\frac{AA_{\eta}}{A^2+B^2} = \frac{\sinh^2(\xi)\sin(\eta)\cos(\eta)\left[\cosh^2(\xi)+\sin^2(\eta)\right]}{\left\{\sinh^2(\xi)+\cos^2(\eta)\right\}^2}, \tag{A16}$$

$$\frac{BA_{\eta}}{A^2+B^2} = \frac{\sinh(\xi)\cosh(\xi)\cos^2(\eta)\left[\cosh^2(\xi)+\sin^2(\eta)\right]}{\left\{\sinh^2(\xi)+\cos^2(\eta)\right\}^2}, \tag{A17}$$

$$\frac{AB_{\xi}}{A^2+B^2} = -\frac{\sinh^2(\xi)\cos(\eta)\sin(\eta)\left[\sin^2(\eta)+\cosh^2(\xi)\right]}{\left\{\sinh^2(\xi)+\cos^2(\eta)\right\}^2}, \tag{A18}$$

$$\frac{BB_{\xi}}{A^2+B^2} = -\frac{\sinh(\xi)\cosh(\xi)\cos^2(\eta)\left[\sin^2(\eta)+\cosh^2(\xi)\right]}{\left\{\sinh^2(\xi)+\cos^2(\eta)\right\}^2}, \tag{A19}$$

$$\frac{AB_{\eta}}{A^2+B^2} = \frac{\sinh(\xi)\cosh(\xi)\sin^2(\eta)\left[\cos^2(\eta)-\sinh^2(\xi)\right]}{\left\{\sinh^2(\xi)+\cos^2(\eta)\right\}^2}, \qquad \text{and,} \tag{A20}$$

$$\frac{BB_{\eta}}{A^2+B^2} = \frac{\cosh^2(\xi)\sin(\eta)\cos(\eta)\left[\cos^2(\eta)-\sinh^2(\xi)\right]}{\left\{\sinh^2(\xi)+\cos^2(\eta)\right\}^2}. \tag{A21}$$

Using (A5) and (A6) along with Equation (2.9b) we obtain,

$$\frac{A}{y} = \frac{\sinh(\xi)}{\left(a^2-b^2\right)\left\{\sinh^2(\xi)+\cos^2(\eta)\right\}\cosh(\xi)}, \qquad \text{and,}$$

$$\frac{B}{y} = \frac{\cos(\eta)}{(a^2 - b^2)\{\sinh^2(\xi) + \cos^2(\eta)\}\sin(\eta)},$$

and using (A13) we have,

$$\frac{A/y}{A^2 + B^2} = \frac{\sinh(\xi)}{\cosh(\xi)} = \tanh(\xi), \qquad \text{and,} \qquad \text{(A22)}$$

$$\frac{B/y}{A^2 + B^2} = \frac{\cos(\eta)}{\sin(\eta)} = \cot(\eta). \qquad \text{(A23)}$$

From Equations (A14)-(A23) C becomes,

$$C = \frac{AA_\xi + BA_\eta + BB_\xi - AB_\eta - A/y}{A^2 + B^2}$$

$$= \frac{1}{\{\sinh^2(\xi) + \cos^2(\eta)\}^2} \begin{bmatrix} \sinh(\xi)\cosh(\xi)\sin^2(\eta)\cos^2(\eta) - \sinh^3(\xi)\cosh(\xi)\sin^2(\eta) \\ + \sinh(\xi)\cosh^3(\xi)\cos^2(\eta) + \sinh(\xi)\cosh(\xi)\cos^2(\eta)\sin^2(\eta) \\ - \sinh(\xi)\cosh(\xi)\cos^2(\eta)\sin^2(\eta) - \sinh(\xi)\cosh^3(\xi)\cos^2(\eta) \\ - \sinh(\xi)\cosh(\xi)\sin^2(\eta)\cos^2(\eta) + \sinh^3(\xi)\cosh(\xi)\sin^2(\eta) \end{bmatrix}$$

$$- \tanh(\xi)$$

$$\Rightarrow C = -\tanh(\xi). \qquad \text{(A24)}$$

From Equations (A14)-(A23) D becomes,

$$D = \frac{AB_\xi + BB_\eta - BA_\xi + AA_\eta - B/y}{A^2 + B^2}$$

$$= \frac{1}{\{\sinh^2(\xi) + \cos^2(\eta)\}^2} \begin{bmatrix} -\sinh^2(\xi)\cos(\eta)\sin^3(\eta) - \sinh^2(\xi)\cosh^2(\xi)\cos(\eta)\sin(\eta) \\ + \cosh^2(\xi)\sin(\eta)\cos^3(\eta) - \sinh^2(\xi)\cosh^2(\xi)\sin(\eta)\cos(\eta) \\ - \cosh^2(\xi)\cos^3(\eta)\sin(\eta) + \cosh^2(\xi)\sinh^2(\xi)\cos(\eta)\sin(\eta) \\ + \sinh^2(\xi)\cosh^2(\xi)\sin(\eta)\cos(\eta) + \sinh^2(\xi)\sin^3(\eta)\cos(\eta) \end{bmatrix}$$

$$- \cot(\eta)$$

$$\Rightarrow D = -\cot(\eta). \qquad \text{(A25)}$$

Using (A25) we find,

$$\frac{2D\sin(\eta)\cos(\eta) + 2\cos(2\eta)}{\sin^2(\eta)} = \frac{-2\cot(\eta)\sin(\eta)\cos(\eta) + 2\cos(2\eta)}{\sin^2(\eta)}$$

$$= \frac{-2\cos^2(\eta) + 2\cos^2(\eta) - 2\sin^2(\eta)}{\sin^2(\eta)} = -2\,. \quad \text{(A26)}$$

Substituting (A24) and (A26) into (A8) gives,

$$F'' - \tanh(\xi)F' - 2F = 0\,,$$

$$\Rightarrow F''(\xi)\cosh(\xi) - F'(\xi)\sinh(\xi) - 2F(\xi)\cosh(\xi) = 0\,.$$

A2. Numerical schemes for skipping stones

Below is the Maple coding for a square stone:

```
> restart;with(plots):
```
Parameters
```
> U:=2.1:
> alpha:=Pi/9:r:=0.05:h:=0.00275:
> m:=evalf(2.7*r^2*h):
> beta[0]:=Pi/9:
```
Numerical Scheme Variables
```
> h:=0.0001:N:=7000:
```
Fixed Constants
```
> G:=9.8:rho:=1:y[0]:=0:x[0]:=0:u[0]:=U*cos(beta[0]):v[0]:=-
U*sin(beta[0]):t[0]:=0:
```
Equations
```
> f:=(F,K)->-F*K*sin(alpha)/m:
> g:=(F,K)->K*F*cos(alpha)/m-G:
> e:=v->v:x:=u->u:
```
Procedure
```
> for j from 0 to N do:
>   if y[j]<=0 then K:=1 else K:=0 fi;
>     if y[j]<=0 then
>       if -y[j]<evalf(r*sin(alpha)) then S:=-r*y[j]/sin(alpha)
>       else S:=0 fi:
>     else S:=0 fi:
>   F:=0.5*rho*U^2*S*sin(alpha+beta[j]):
>   c[1]:=h*e(v[j]):
>   c[2]:=h*e(v[j]+c[1]/2):
>   c[3]:=h*e(v[j]+c[2]/2):
>   c[4]:=h*e(v[j]+c[3]):
>   b[1]:=h*w(u[j]):
>   b[2]:=h*w(u[j]+b[1]/2):
>   b[3]:=h*w(u[j]+b[2]/2):
>   b[4]:=h*w(u[j]+b[3]):
>   y[j+1]:=evalf(y[j]+(1/6)*(c[1]+2*c[2]+2*c[3]+c[4])):
>   x[j+1]:=evalf(x[j]+(1/6)*(b[1]+2*b[2]+2*b[3]+b[4])):
>   u[j+1]:=evalf(u[j]+h*f(F,K)):
>   v[j+1]:=evalf(v[j]+h*g(F,K)):
>   t[j+1]:=t[j]+h:
>   U:=evalf(sqrt(u[j+1]^2+v[j+1]^2)):
>   beta[j+1]:=evalf(arctan(-v[j+1]/u[j+1])):
> end:
```
Solutions
```
> Data:=seq([x[j],y[j]],j=0..N):
> PathPlot:=listplot([Data]):display(PathPlot);
```

For a circular stone the Maple coding is the same as above except the blue highlight is replaced with:

```
S:=r^2*(arccos(1+y[j]/sin(alpha)/r)-(1+y[j]/sin(alpha)/r)*sqrt(1-
(1+y[j]/sin(alpha)/r)^2)):
```

References

[1] ACHESON, D. J. 1990. *Elementary Fluid Dynamics*. Oxford University Press. p 66.

[2] BATCHELOR, G. K. 2000. *An Introduction to Fluid Dynamics*. Cambridge University Press.

[3] BOCQUET, L. 2003. The physics of stone skipping. *Am. J. Phys*, vol 71, pp. 150-155.

[4] CLANET, C., HERSEN, F., and BOCQUET, L. 2004. Secrets of successful stone-skipping. *Nature*, vol 427, p. 29.

[5] COOKER and PEREGRINE. 1995. {fill in reference}

[6] GODA, Y. 2000. *Random Seas and Design of Maritime Structures*. 2nd Edition. World Scientific Publishing Co. Pte. Ltd.

[7] HANNAH, J., and HILLIER, M. J. 1995. *Applied Mechanics*. 3rd Edition. Pearson Education Ltd. p 390.

[8] HOWISON, S. D. 2006. Personal communication.

[9] HUTCHINGS, I. 1978. Bouncing Bombs of the Second World War. *New Scientist*, 2nd March, pp. 563-567.

[10] JACQUES, I., and JUDD, C., 1987. *Numerical Analysis*. London: Chapman and Hall Ltd.

[11] KING, A. C., and NEEDHAM, D. J. 1994. The initial development of a jet caused by fluid, body and free-surface interaction. *J. Fluid Mech*, vol 268, pp. 89-101.

[12] KOROBKIN, A., and PUKHNACHOV, V. 1988. Initial stage of water impact. *Ann. Rev. Fluid Mech*, vol 20, pp. 159-185.

[13] KOROBKIN, A. 1996. Global characteristics of jet impact. *J. Fluid Mech*, vol. 307, pp.63-84.

[14] KOROBKIN, A. 1999. Shallow-water impact problems. *Journal of Engineering Mathematics*, vol 35, pp. 233-250.

[15] KURT STEINER, GUINNESS WORLD RECORD STONE SKIPPER, 2006. *Stone Skipping* [online]. Available at: <URL:http//www.pastoneskipping.com/steiner.htm>

[16] LANDAU, L. D., and LIFSHITZ, E. M. 1959. *Fluid Mechanics*, pp. 168-175. Pergamon.

[17] MILOH, T., and SHUKRON. Y. 1991. Ricochet Off Water of Spherical Projectiles. *Journal of Ship Research*, vol 35, no 2, pp. 91-100.

[18] OFFICIAL WEBSITE OF THE MISSGC, 2006. *Stone Skipping* [online]. Available at : <URL:http//www.stoneskipping.com/HomePage.htm>

[19] ROSELLINI, L., HERSEN, F., CLANET, C., and BOCQUET, L. 2005. *Skipping Stones*. J. Fluid Mech, vol 543, pp. 137-146.

[20] VON KARMAN, TH. 1929. The impact of sea planes during landing. *NACA Tech. Note* 321.

[21] ZHAO, R., and FALTINSEN, O. 1993. Water entry of two-dimensional bodies. *J. Fluid Mech*, vol. 246, pp. 593-612.